



Article

# Inverse Regulation of Lipocalin-2/24p3 Receptor/SLC22A17 and Lipocalin-2 Expression by Tonicity, NFAT5/TonEBP and Arginine Vasopressin in Mouse Cortical Collecting Duct Cells mCCD(cl.1): Implications for Osmotolerance

Stephanie Probst <sup>1,†</sup>, Bettina Scharner <sup>1,†</sup>, Ruairi McErlean <sup>1,2</sup>, Wing-Kee Lee <sup>1</sup> and Frank Thévenod <sup>1,\*</sup>

<sup>1</sup> Department of Physiology, Pathophysiology & Toxicology and ZBAF (Centre for Biomedical Education and Research), Faculty of Health, School of Medicine, Witten/Herdecke University, Stockumer Str 12 (Thyssenhaus), D-58453 Witten, Germany; Stephanie.Probst@uni-wh.de (S.P.); Bettina.Scharner@uni-wh.de (B.S.); ruairi.mcerlean@student.manchester.ac.uk (R.M.); Wing-Kee.Lee@uni-wh.de (W.-K.L.)

<sup>2</sup> Faculty of Biology, Medicine and Health, School of Biological Sciences, University of Manchester, Oxford Rd, Manchester M13 9PL, UK

\* Correspondence: frank.thevenod@uni-wh.de

† These authors contributed equally to the work.

Received: 3 September 2019; Accepted: 22 October 2019; Published: 30 October 2019



**Abstract:** The rodent collecting duct (CD) expresses a 24p3/NGAL/lipocalin-2 (LCN2) receptor (SLC22A17) apically, possibly to mediate high-affinity reabsorption of filtered proteins by endocytosis, although its functions remain uncertain. Recently, we showed that hyperosmolarity/-tonicity upregulates SLC22A17 in cultured mouse inner-medullary CD cells, whereas activation of toll-like receptor 4 (TLR4), via bacterial lipopolysaccharides (LPS), downregulates SLC22A17. This is similar to the upregulation of *Aqp2* by hyperosmolarity/-tonicity and arginine vasopressin (AVP), and downregulation by TLR4 signaling, which occur via the transcription factors NFAT5 (TonEBP or OREBP), cAMP-responsive element binding protein (CREB), and nuclear factor-kappa B, respectively. The aim of the study was to determine the effects of osmolarity/tonicity and AVP, and their associated signaling pathways, on the expression of SLC22A17 and its ligand, LCN2, in the mouse (m) cortical collecting duct cell line mCCD(cl.1). Normosmolarity/-tonicity corresponded to 300 mosmol/L, whereas the addition of 50–100 mmol/L NaCl for up to 72 h induced hyperosmolarity/-tonicity (400–500 mosmol/L). RT-PCR, qPCR, immunoblotting and immunofluorescence microscopy detected *Slc22a17*/SLC22A17 and *Lcn2*/LCN2 expression. RNAi silenced *Nfat5*, and the pharmacological agent 666-15 blocked CREB. Activation of TLR4 was induced with LPS. Similar to *Aqp2*, hyperosmotic/-tonic media and AVP upregulated *Slc22a17*/SLC22A17, via activation of NFAT5 and CREB, respectively, and LPS/TLR4 signaling downregulated *Slc22a17*/SLC22A17. Conversely, though NFAT5 mediated the hyperosmolarity/-tonicity induced downregulation of *Lcn2*/LCN2 expression, AVP reduced *Lcn2*/LCN2 expression and predominantly apical LCN2 secretion, evoked by LPS, through a posttranslational mode of action that was independent of CREB signaling. In conclusion, the hyperosmotic/-tonic upregulation of SLC22A17 in mCCD(cl.1) cells, via NFAT5, and by AVP, via CREB, suggests that SLC22A17 contributes to adaptive osmotolerance, whereas LCN2 downregulation could counteract increased proliferation and permanent damage of osmotically stressed cells.

**Keywords:** kidney; hypertonicity; osmotic stress; lipocalin-2; lipocalin-2 receptor; lipopolysaccharide; TonEBP; CREB

## 1. Introduction

The chief site of urine concentration is in the collecting duct (CD) system [1]. There, the major effector in the regulation of renal water excretion is the antidiuretic hormone arginine vasopressin (AVP), which binds to the AVP type-2 receptor (V2R) and signals through cAMP [2]. AVP facilitates urinary concentration in the medullary and cortical CD of the kidneys, by increasing CD water permeability through the enhancement of aquaporin-2 (AQP2) water channel incorporation in the luminal membrane of principal cells, permitting water to flow passively along the osmotic gradient, from the tubule lumen to the interstitium [3]. AVP stimulation activates adenylyl cyclase, which results in increased cytosolic cAMP concentration and subsequent protein kinase A (PKA) activation. This, in turn, triggers the trafficking of intracellular storage vesicles expressing AQP2 to the luminal plasma membrane, within a range of 10–30 min (short-term regulation), and also increases *Aqp2* gene transcription, via the increased activity of cAMP-responsive element binding protein (CREB) and AP-1 [4–6], over a time period ranging from hours to days (long-term regulation).

For AVP to exert its effects on water transport in the CD, axial cortico–papillary osmotic gradients need to be generated through the accumulation of high interstitial concentrations of NaCl (300–400 mmol/L) and urea (> 600 mmol/L) [7,8]. Na<sup>+</sup> reabsorption in the thick ascending limb results in a renal cortico–papillary osmotic gradient. However, this gradient exposes renal cells to substantial osmotic stress by causing numerous perturbations (reviewed in [9]). Cells can respond to high osmotic stress by activating adaptive mechanisms through various pathways that activate the transcription factor NFAT5 (also known as tonicity-named responsive enhancer binding protein (TonEBP or OREBP)), culminating in the accumulation of organic osmolytes and increased expression of heat shock proteins (reviewed in [9]). In addition to AVP, extracellular tonicity is pivotal in determining AQP2 abundance, through the activation of NFAT5, which boosts AVP-induced transcriptional activation of *Aqp2*. Conversely, activation of the NF-κB transcriptional factor by pro-inflammatory signals reduces *Aqp2* gene transcription (reviewed in [3,10]).

The CD is a site of ascending urinary tract infections (UTI). Lipocalin-2 (LCN2; also NGAL [human] or siderocalin/24p3 [rodent]) binds Fe<sup>3+</sup> through association with bacterial siderophores, hence it plays an important role in innate antibacterial immunity [11]. Activation of the Toll-like receptor 4 (TLR4) on CD cells, by the bacterial wall component lipopolysaccharide (LPS), has been shown to induce LCN2 secretion to combat urinary bacterial infections [12]. A receptor for LCN2 (LCN2-R/SLC22A17/24p3-R) has been cloned (MM ~60kDa) [13], and is expressed in the apical membrane of distal convoluted tubules and CD [14]. Experimental evidence in cultured cells and in vivo [14,15] indicates that SLC22A17 is a high-affinity receptor, involved in protein endocytosis in the distal nephron [16]. In fact, the affinity of SLC22A17 to filtered proteins, such as LCN2 or metallothionein, is ~1000x higher than that of megalin [14] (reviewed in [16,17]), the high-capacity receptor for endocytic reabsorption of filtered proteins in the proximal tubule [18].

Our understanding of the physiological regulation of SLC22A17 and LCN2 expression in vivo is poor. Recent data, obtained by deep sequencing in micro-dissected nephrons, showed the highest SLC22A17 expression levels in the rat inner medullary CD (IMCD) compared to other nephron segments, whereas LCN2 levels were negligible [19]. Abundant localization of SLC22A17 in the CD [14] strongly implies a relationship with the hypertonic environment, and possibly regulation by AVP. Our recent data in a mouse IMCD cell line (mIMCD<sub>3</sub>) evidenced *Slc22a17*/SLC22A17 upregulation and *Lcn2*/LCN2 downregulation, induced by hyperosmolarity/-tonicity, suggesting adaptive osmotolerant survival, whereas *Lcn2*/LCN2 upregulation and *Slc22a17*/SLC22A17 downregulation, via TLR4, indicated protection against bacterial infections [20].

In the present study, the role of increased osmolarity/tonicity on SLC22A17 and LCN2 expression was investigated in the mouse cortical CD (CCD) cell line mCCD(cl.1). The data indicate that regulation of SLC22A17 expression is analogous to AQP2, i.e., increased osmolarity/tonicity and AVP induced expression of SLC22A17, via activation of the transcription factors NFAT5 and CREB, respectively, which is counteracted by LPS/TLR4 signaling. Whereas NFAT5 mediates LCN2 downregulation

elicited by hyperosmolarity/-tonicity, AVP reduces LCN2 expression and secretion evoked by LPS, through a posttranslational mode of action. The parallel regulation of AQP2 and SLC22A17 expression in mCCD(cl.1) cells suggest the role of SLC22A17 in vivo in urine concentration and/or osmotic stress adaptation.

## 2. Results

### 2.1. Hyperosmolarity Increases the Expression of *Slc22a17*/SLC22A17 in mCCD(cl.1) Cells

The CD can be separated into the CCD, outer medullary CD (OMCD) and IMCD. Each section of the CD contributes to urine concentration and is also exposed to varying degrees of osmotic stress. As a matter of fact, extracellular osmolarity increases from approximately 300 mosmol/L in the renal cortex, to, maximally, 1200 mosmol/L in the renal medulla. We have previously shown that increased extracellular osmolarity augments abundance of the LCN2 receptor SLC22A17 in a mouse IMCD cell line (mIMCD<sub>3</sub>) [20]. SLC22A17 is expressed apically along the rodent CD [14] as well as in the mCCD(cl.1) cell line [21]. To assess whether the CCD also harbors a similar positive regulatory relationship between extracellular osmolarity and SLC22A17 expression, mCCD(cl.1) cells were exposed to hyperosmotic medium and *Slc22a17* expression was determined. Indeed, increased osmolarity to 400 mosmol/L for 6 h (data not shown) and 12 h induced *Slc22a17* mRNA, as demonstrated by RT-PCR (Figure 1A) and qPCR (Figure 1B). Moreover, hyperosmolarity for 48 h increased plasma membrane expression of SLC22A17 protein (Figure 1C). This was associated with increased protein expression of SLC22A17 in microsomes of mCCD(cl.1) cells, that are enriched via the plasma membrane-located Na<sup>+</sup>/K<sup>+</sup>-ATPase (Figure 1D). In addition, Na<sup>+</sup>/K<sup>+</sup>-ATPase was also upregulated in cells exposed to hyperosmotic media, which indicates that an adaptive osmoprotective response to hyperosmolarity has been engaged [9]. In contrast, the ligand of SLC22A17, *Lcn2*, was downregulated by hyperosmolarity by RT-PCR (Figure 1E) and qPCR (Figure 1F), which is in line with recent data in mIMCD<sub>3</sub> cells [20]. Overall, these data indicate that hyperosmolarity regulates *Slc22a17*/SLC22A17 expression in the CCD cell line mCCD(cl.1), whereas the expression of its natural ligand *Lcn2* is reduced, recapitulating the observations made in IMCD cells [20].

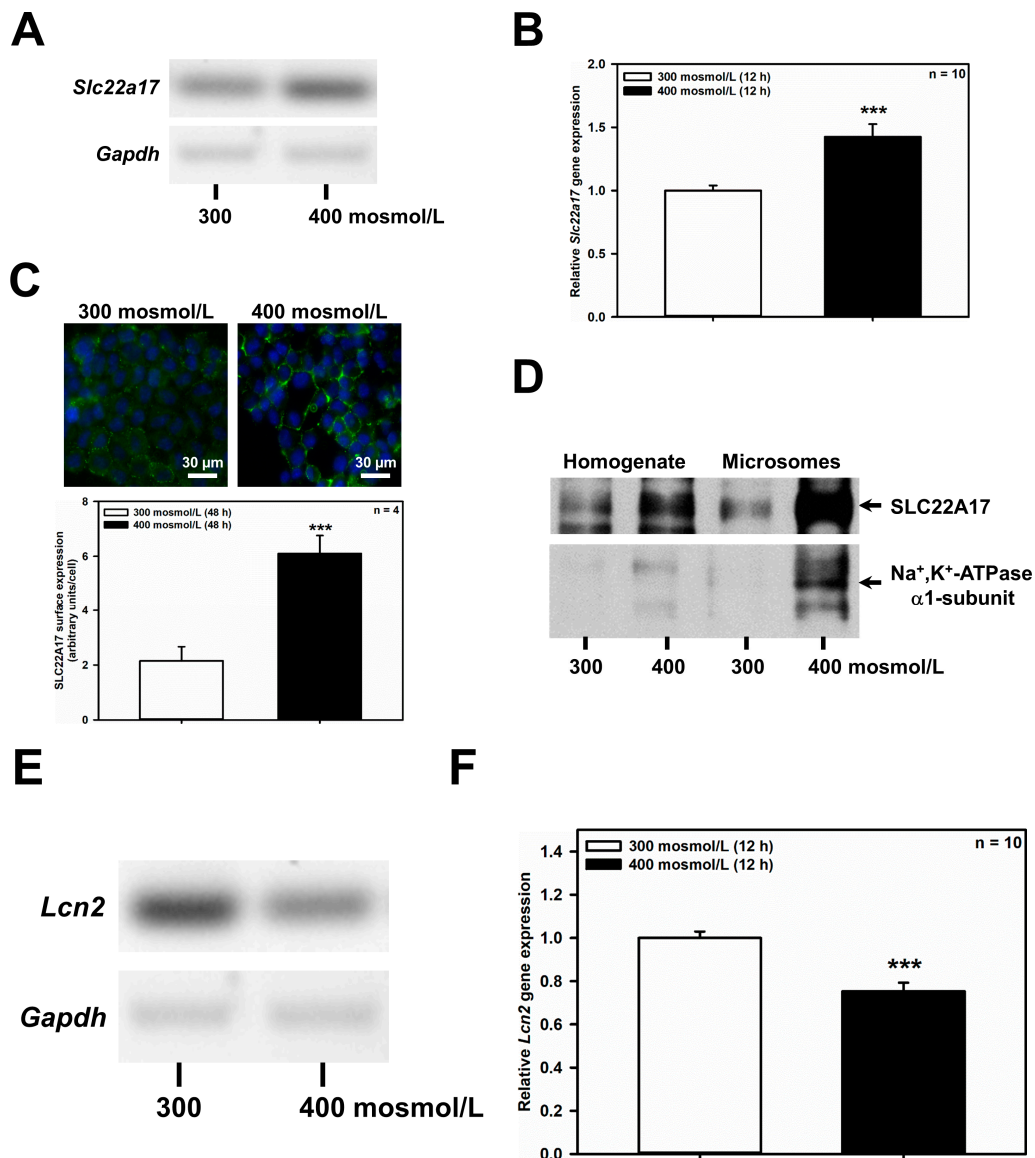


**Figure 1.** Hyperosmolarity increases *Slc22a17*/SLC22A17 expression and decreases *Lcn2* expression in mCCD(cl.1) cells. (A) RT-PCR analysis of *Slc22a17* and *Gapdh* mRNA in mCCD(cl.1) cells exposed to 300 mosmol/L (normosmolarity) or 400 mosmol/L (hyperosmolarity) for 12 h. The experiment is similar to three others. (B) Expression levels of *Slc22a17* mRNA by qPCR in mCCD(cl.1) cells exposed to norm- or hyperosmotic media for 12 h. Means  $\pm$  SEM of 10 experiments are shown. Data normalized to the expression of *Gapdh* and *Actb* show relative expression levels of *Slc22a17* under hyperosmotic conditions, where expression at 300 mosmol/L is set to 1.0. Statistics compare hyper- to normosmolarity by unpaired *t*-test. (C) Surface expression of SLC22A17 in mCCD(cl.1) cells exposed to norm- or hyperosmotic media for 48 h. SLC22A17 is detected by live immunofluorescence microscopy of non-fixed and non-permeabilized cells with a SLC22A17 antibody directed against the extracellular N-terminus. Hoechst 33342 counterstains nuclei. Means  $\pm$  SEM of four experiments and comparison of the two osmotic conditions by unpaired *t*-test are shown. a.u. = arbitrary units. (D) Immunoblotting of homogenate and microsomes enriched in plasma membranes from mCCD(cl.1) cells grown for 72 h in norm- or hyperosmotic media. SLC22A17 is at the expected molecular mass of ~62 kDa. The  $\alpha$ 1-subunit of Na<sup>+</sup>, K<sup>+</sup>-ATPase, a plasma membrane marker, is enriched in microsomes and upregulated in cells exposed to hyperosmolarity. The experiment is representative of three similar ones. (E) RT-PCR analysis of *Lcn2* and *Gapdh* mRNA in mCCD(cl.1) cells exposed to 300–400 mosmol/L media for 12 h. The experiment is typical of three similar ones. (F) Expression levels of *Lcn2* mRNA by qPCR in mCCD(cl.1) cells exposed to 300–400 mosmol/L media for 12 h. Means  $\pm$  SEM of 10 experiments are shown. Data

normalized to the expression of *Gapdh* and *Actb* show relative expression levels of *Lcn2* under hyperosmotic conditions, where expression at 300 mosmol/L is set to 1.0. Statistics compare the two osmotic conditions by unpaired *t*-test. For a definition of asterisks, see “statistics” in the Methods.

2.2. Hypertonicity Dependent Upregulation of *Slc22a17/SLC22A17* and Downregulation of *Lcn2/LCN2* are Mediated by NFAT5 in mCCD(cl.1) Cells

Increased extracellular osmolarity has previously been shown to increase abundance of the water channel *Aqp2* *in vivo* [22,23], and in the mouse renal CD principal cell line mpkCCDcl4 (reviewed in [3,10]), and depends on increased nuclear activity of the transcription factor NFAT5 (TonEBP/OREBP) [24], which is also affected by osmolarity *in vivo* [25]. These findings were confirmed in the mCCD(cl.1) cell line: hyperosmolarity of 400 mosmol/L for 24 h upregulated *Aqp2* mRNA by RT-PCR (Figure 2A), and qPCR (Figure 2B), slightly increased NFAT5 (Figure 2C), suggesting the slow induction of NFAT5 protein [26,27], and hyperosmolarity of 400–500 mosmol/L induced translocation of cytosolic NFAT5 to nuclei (Figure 2D). To investigate whether the upregulation of *Aqp2* by hyperosmolarity is also mediated by NFAT5 in mCCD(cl.1) cells, RNAi was performed, using siRNAs against *Nfat5*, which efficiently abolished the hyperosmolarity-induced increase in both *Nfat5* mRNA (Figure 2E) and NFAT5 protein (Figure 2C) levels. Accordingly, as expected, *Nfat5* silencing almost abolished the induction of *Aqp2* mRNA elicited by hyperosmolarity (Figure 2F).

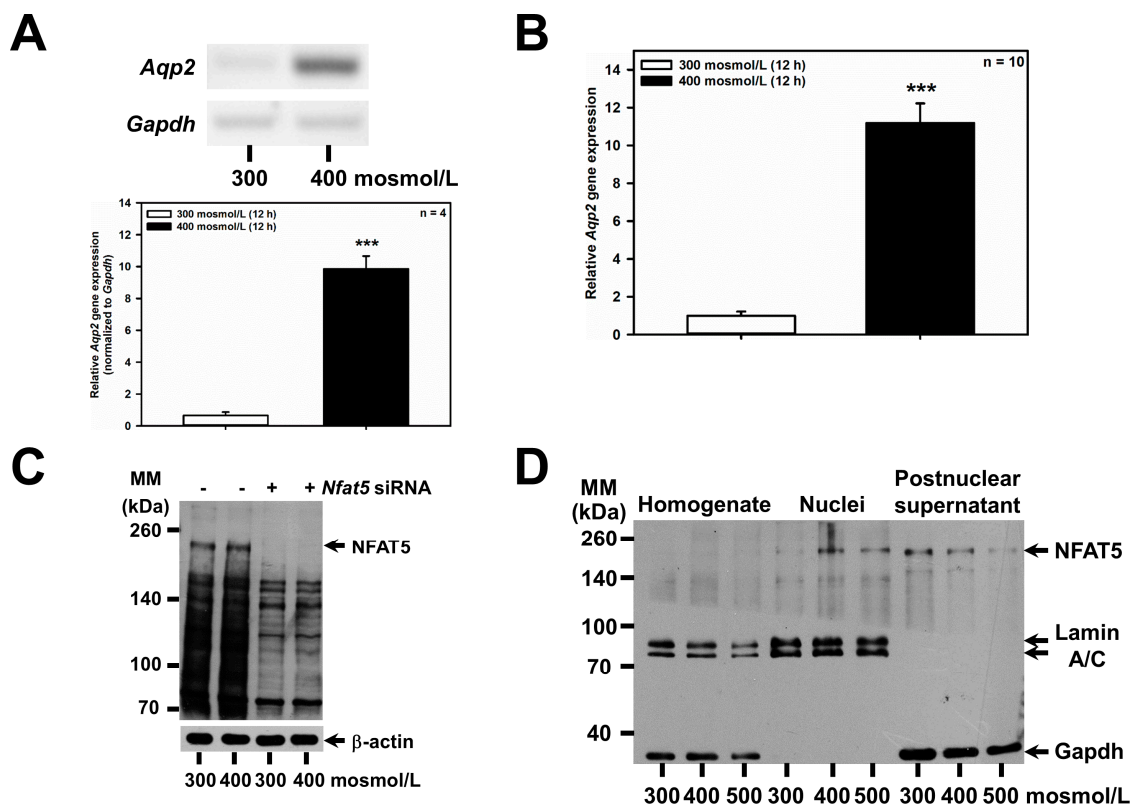
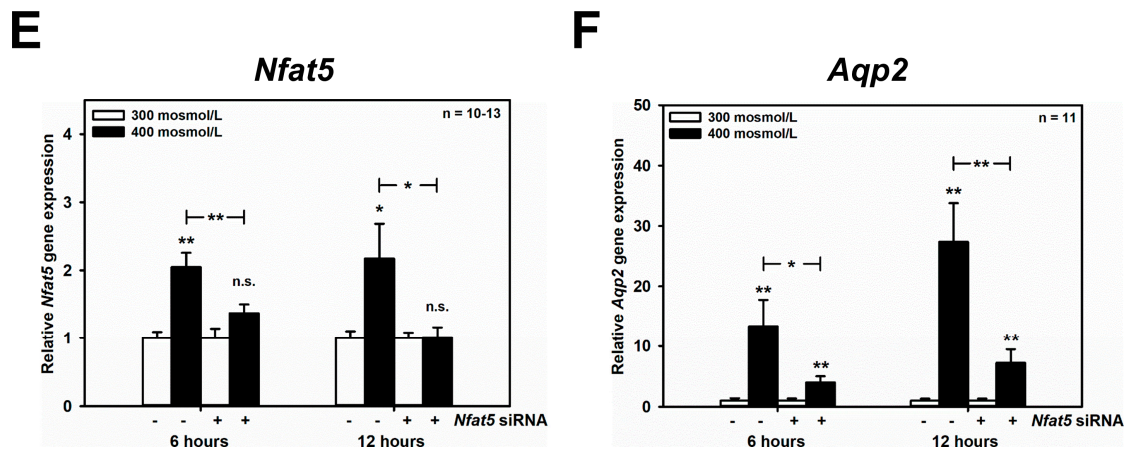
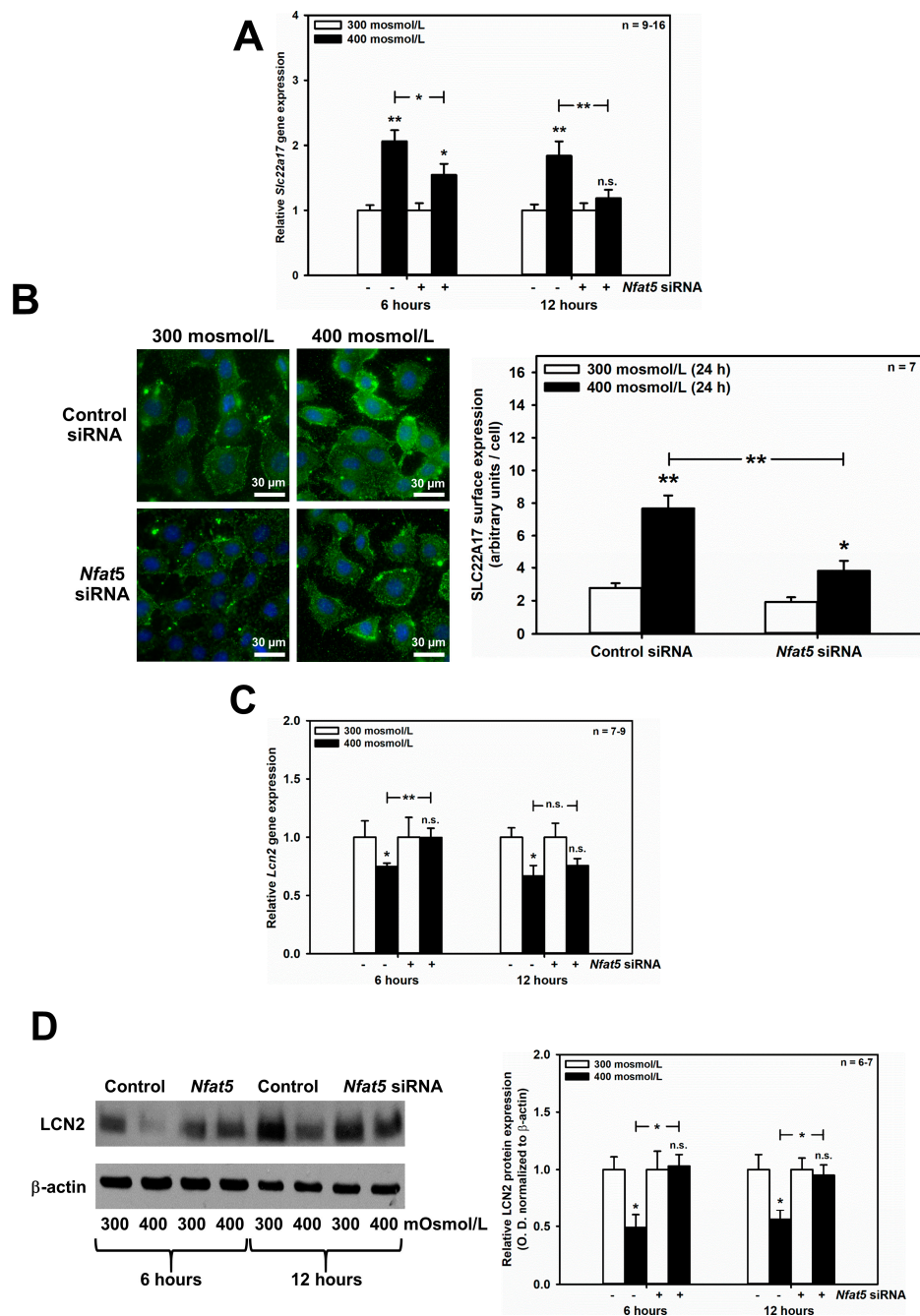


Figure 2. Cont.



**Figure 2.** *Aqp2* upregulation induced by hyperosmolarity is mediated by NFAT5 in mCCD(cl.1) cells. (A) Expression levels of *Aqp2* mRNA by RT-PCR in mCCD(cl.1) cells exposed to 300–400 mosmol/L for 12 h. *Aqp2* mRNA expression was normalized to *Gapdh*, and expression levels at 300 mosmol/L are set to 1.0. Data show means  $\pm$  SEM of four experiments. Statistical analysis compares hyper- to normosmolarity by unpaired *t*-test. (B) Expression levels of *Aqp2* mRNA by qPCR in mCCD(cl.1) cells exposed to 300–400 mosmol/L. Means  $\pm$  SEM of 10 experiments are shown. Data normalized to the expression of *Gapdh* and *Actb* show relative expression levels of *Aqp2* under hyperosmotic conditions, where expression at 300 mosmol/L is set to 1.0. Statistics compare hyper- to normosmolarity by unpaired *t*-test. (C) mCCD(cl.1) cells were transfected with control or *Nfat5* siRNA by electroporation and cultured, as described above, prior to a medium change to 300 and 400 mosmol/L for an additional 24 h, and immunoblotting.  $\beta$ -actin serves as a loading control. The blot is typical of three similar ones. MM = molecular mass. (D) Distribution of NFAT5 in homogenate, nuclei and postnuclear supernatant of mCCD(cl.1) cells exposed to 300–500 mosmol/L for 24 h prior to homogenization, subcellular fractionation and immunoblotting of NFAT5. Lamin A/C and GAPDH are markers of nuclei and cytosol, respectively. The immunoblot is typical of three different blots. MM = molecular mass. (E,F) mCCD(cl.1) cells are transfected with siRNA against *Nfat5* or control siRNA by electroporation. Then cells are seeded in 25 cm<sup>2</sup> flasks and grown for 24 h, prior to a medium change to 300 or 400 mosmol/L and incubation for an additional 6–12 h. Expression levels of *Nfat5* (E) and *Aqp2* mRNA (F) are determined by qPCR, as described above. Statistical analysis shows means  $\pm$  SEM of 10–13 experiments and compares experimental conditions by one-way ANOVA. n.s. = not significant. For a definition of asterisks, see “statistics” in the Methods.

Since the central response pathway to changes in tonicity is NFAT5, we hypothesized that SLC22A17 and its ligand, LCN2, could be regulated by NFAT5 when extracellular osmolarity rises. Strikingly, induction of *Slc22a17* mRNA by hyperosmolarity was significantly reduced by *Nfat5* silencing after 6–12 h (Figure 3A), and expression of the SLC22A17 protein at the surface of mCCD(cl.1) cells was significantly decreased after 24 h hyperosmolarity (Figure 3B). In contrast, *Nfat5* silencing reversed the downregulation of *Lcn2* mRNA expression induced by hyperosmolarity. Figure 3C shows that hyperosmolarity induced an early decrease of *Lcn2* mRNA at 6 and 12 h, which was significantly reversed by *Nfat5* silencing at 6 h, and confirmed at the protein level by immunoblotting of LCN2 (Figure 3D). Hence, the transcription factor NFAT5, which regulates the expression of genes involved in osmotic stress, is largely responsible for up- and downregulation of *Slc22a17*/SLC22A17 and *Lcn2*/LCN2, respectively.



**Figure 3.** NFAT5 mediates the effects of hyperosmolarity on *Slc22a17*/SLC22A17 and *Lcn2*/LCN2 expression in mCCD(cl.1) cells. (A,C) mCCD(cl.1) cells were transfected with control or *Nfat5* siRNA by electroporation, and cultured as described in the Methods, prior to a medium change to 300 or 400 mosmol/L and incubation for additional 6–12 h. Expression levels of *Slc22a17* (A) and *Lcn2* (C) mRNA were detected by qPCR, as described in Figure 1. Statistical analysis shows means  $\pm$  SEM of 7–16 experiments and compares experimental conditions by one-way ANOVA. n.s. = not significant. (B) Surface expression of SLC22A17 was determined in mCCD(cl.1) cells, transfected with siRNA against *Nfat5*, or control siRNA, by electroporation. Cells are exposed to 300 or 400 mosmol/L for an additional 24 h. Plasma membrane SLC22A17 is detected, as described in Figure 1. Hoechst 33342 counterstains nuclei. Statistical analysis shows means  $\pm$  SEM of seven experiments and compares the experimental conditions by one-way ANOVA. n.s. = not significant. (D) Immunoblotting of cellular LCN2 protein in mCCD(cl.1) cells, transfected with siRNA against *Nfat5*, or control siRNA, by electroporation. Incubation of cells occurs in 300 or 400 mosmol/L media for an additional 6–12 h, prior

to immunoblotting. Data show cellular LCN2 protein expression normalized to  $\beta$ -actin as means  $\pm$  SEM of 6–7 experiments, where expression at 300 mosmol/L is set to 1.0. Statistical analysis compares the experimental conditions by one-way ANOVA. n.s. = not significant. For a definition of asterisks, see “statistics” in the Methods.

### 2.3. ddAVP Upregulates *Slc22a17*/SLC22A17 via cAMP/CREB Signaling in mCCD(cl.1) Cells

In addition to hyperosmolarity, the V2R also increases AQP2 protein abundance, to facilitate urinary concentration in the CCD and MCD [28,29], through a cAMP-responsive element (CRE) located in the *Aqp2* promoter, leading to AVP-induced *Aqp2* transcription [4–6]. This mechanism has been reported in mpkCCDcl4 cells [30,31]. Analogously, when mCCD(cl.1) cells were exposed to the specific V2R agonist ddAVP (10 nM) for 24 h in an isotonic medium, *Aqp2* mRNA increased  $5.85 \pm 0.71$ -fold, and this effect was significantly reduced to  $2.60 \pm 0.29$  (means  $\pm$  SEM of 7–11 experiments) by the potent inhibitor of CREB-mediated gene transcription, 666-15 (100–250 nM) [32] (Figure 4A). Notably, ddAVP slightly, but significantly upregulated *Slc22a17* mRNA ( $1.38 \pm 0.06$ -fold;  $n = 7$ –11) in a 666-15 sensitive-manner (Figure 4A). The latter results were further confirmed at the protein level by quantifying surface expression of SLC22A17 protein in mCCD(cl.1) cells, treated exactly as described for the qPCR data shown in Figure 4A. Figure 4B shows that ddAVP increased SLC22A17 surface expression about two-fold, and the role of CREB activation was demonstrated by a significant reduction in SLC22A17 surface expression, by preincubation with 666-15 (Figure 4B). Consequently, gene regulatory mechanisms for SLC22A17, via the transcription factors NFAT5 and CREB, in response to osmotic stress, parallels that of *Aqp2*.

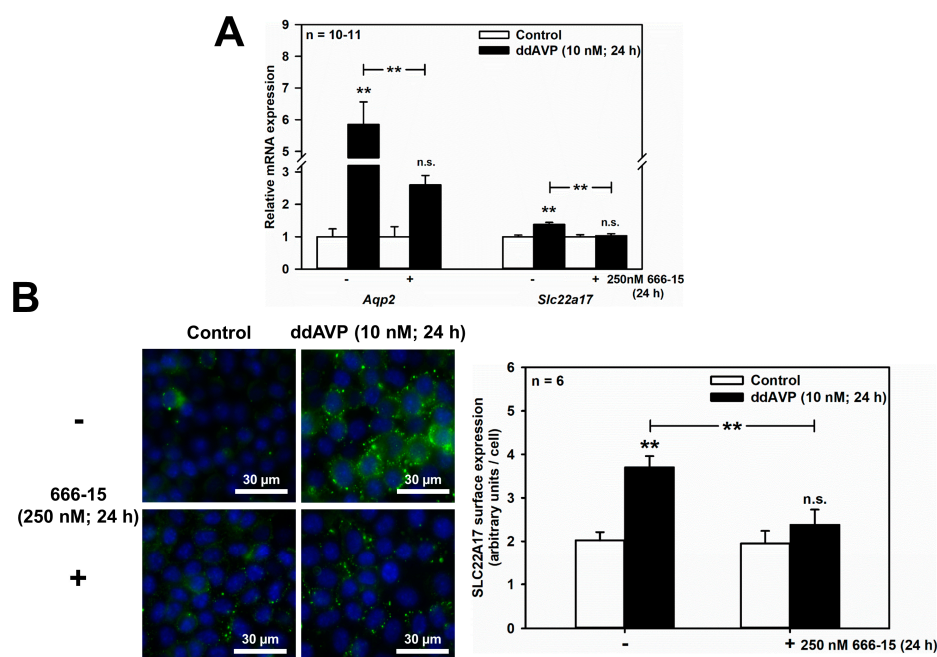


**Figure 4.** ddAVP increases *Slc22a17*/SLC22A17 expression through CREB activation in mCCD(cl.1) cells. (A) Expression levels of *Aqp2* and *Slc22a17* mRNA by qPCR, in cells treated with ddAVP  $\pm$  the CREB inhibitor 666-15, and analyzed and calculated as described in Figure 1. Data are means  $\pm$  SEM of 10–11 experiments. Statistical analysis compares relative expression levels of *Aqp2* or *Slc22a17* in controls and ddAVP-treated cells  $\pm$  666-15 by one-way ANOVA. n.s. = not significant. (B) Surface expression of SLC22A17 in cells treated with ddAVP  $\pm$  666-15. Staining of non-fixed and non-permeabilized cells grown on glass coverslips was performed using a SLC22A17 antibody, directed against the extracellular N-terminus. Hoechst 33342 counterstains nuclei. Statistical analysis shows the means  $\pm$  SEM of six experiments, and compares the four experimental conditions by one-way ANOVA. n.s. = not significant. For a definition of asterisks, see “statistics” in the Methods.

#### 2.4. LPS Downregulates *Slc22a17*/SLC22A17 and Upregulates *Lcn2*/LCN2 in mCCD(cl.1) Cells

The renal CD is susceptible to bacterial infections that can ascend from the lower urinary tract during UTIs. The activation of TLR4 [33] in collecting ducts [34], mediated by NF- $\kappa$ B-mediated signaling [35], via bacterial LPS, has been shown in our earlier work to induce LCN2 upregulation and SLC22A17 downregulation in mIMCD<sub>3</sub> cells, and suggested to protect IMCD cells against bacterial infections, and prevent autocrine death induction by LCN2 [20]. Here we investigated whether LPS also inhibits SLC22A17 expression in the CCD. When mCCD(cl.1) cells incubated in isotonic medium were exposed to LPS (5  $\mu$ g/mL) for 12 h, *Slc22a17* mRNA was significantly reduced (Figure 5A), as measured by RT-PCR. Similarly, LPS reduced cellular and surface expression of SLC22A17, as well (Figure 5B). LPS at 100 ng/mL for 12 h yielded similar results.

Further corroborating our previous findings in IMCD cells, LPS (5  $\mu$ g/mL for 12 h) significantly stimulated *Lcn2* mRNA expression in mCCD(cl.1) cells (Figure 5C), and increased LCN2 protein expression, when cells were exposed for 18 h to 5  $\mu$ g/mL LPS (Figure 5D,E). Interestingly, LPS exposure time  $\leq$  12 h marginally increased LCN2 secretion. This high LPS concentration of 5  $\mu$ g/mL is saturating, with regard to LCN2 secretion in mCCD(cl.1) cells (Supplementary Figure S1A). It has previously been shown to activate NF- $\kappa$ B dependent TLR4 signaling in cultured mouse CD cell lines, which involves rapid I $\kappa$ B- $\alpha$  degradation [36,37] (Supplementary Figure S1B), as well as in primary CD cells [38] (although additional activation of the non-canonical, TLR4-independent inflammasome pathway cannot be excluded). Secretion of LCN2 occurred predominantly apically, when LPS was applied to both the apical and basolateral compartments of confluent monolayers of mCCD(cl.1) cells grown on transwell filters (Figure 5E). Yet, unstimulated secretion was also predominantly apical (Figure 5E), confirming that constitutive, as well as regulated, LCN2 secretion largely targets the apical plasma membrane, as previously suggested [12].

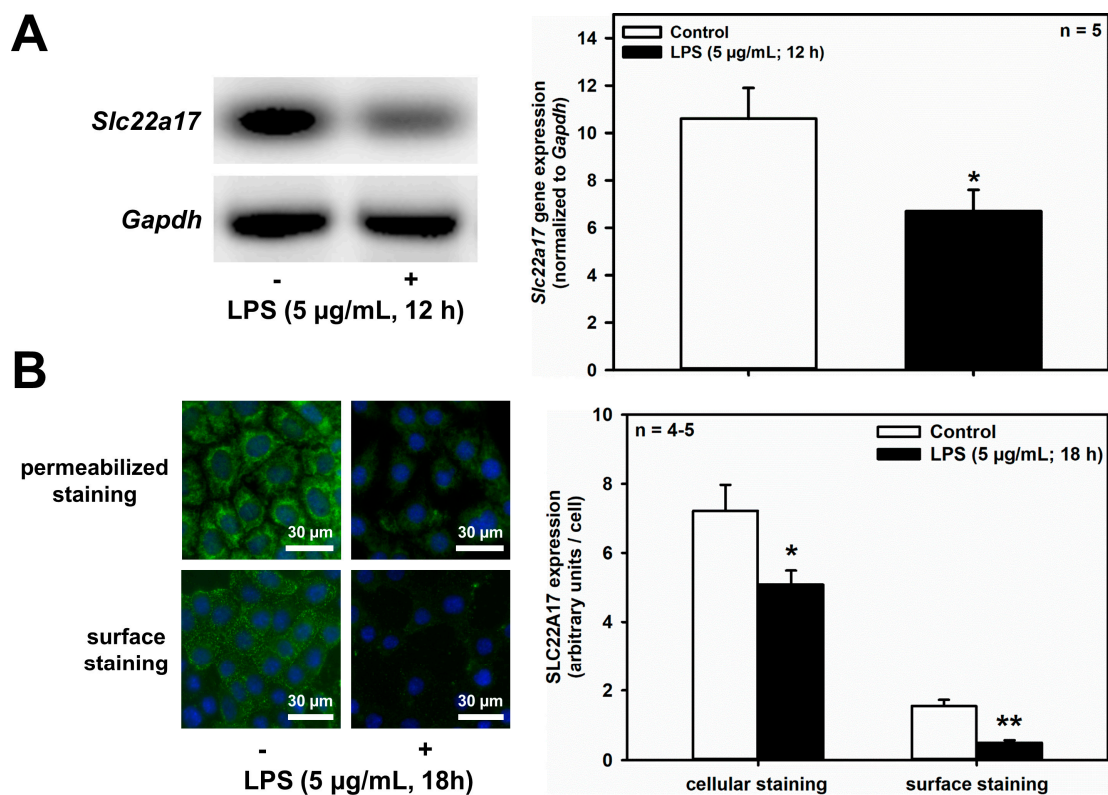
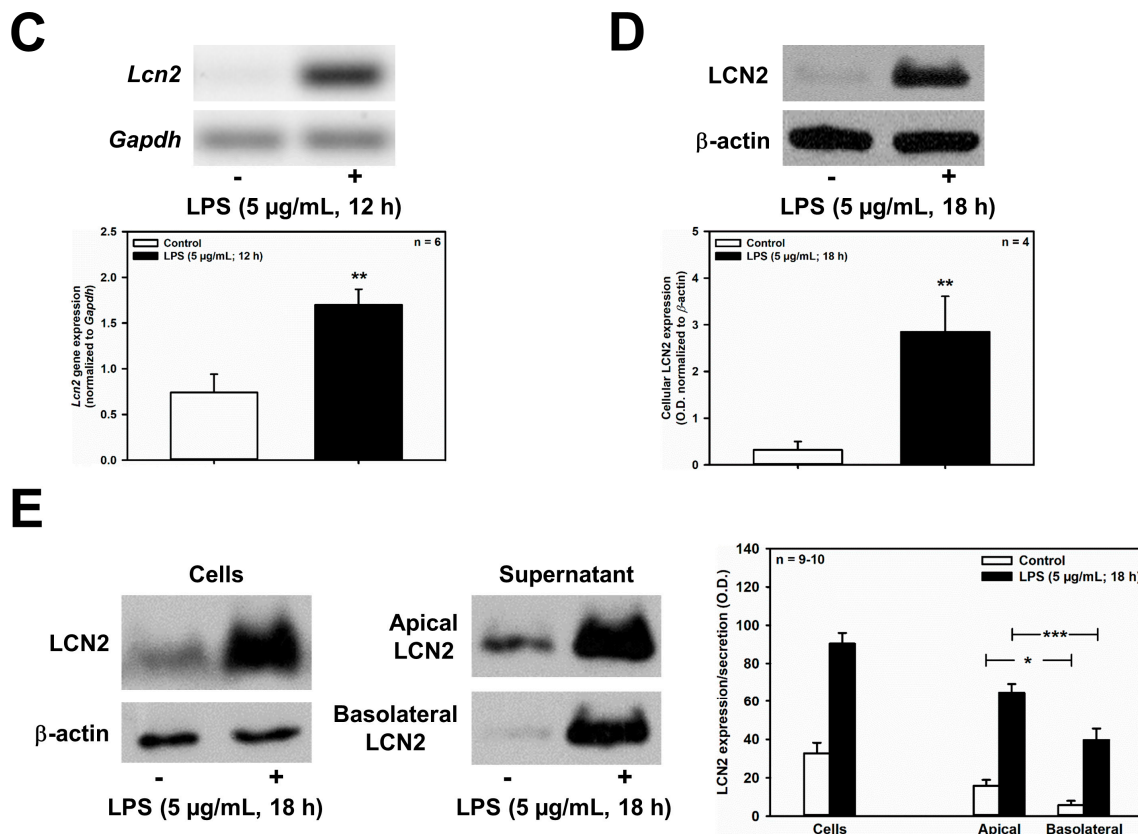


Figure 5. Cont.



**Figure 5.** LPS decreases *Slc22a17*/SLC22A17 expression and increases *Lcn2*/LCN2 expression in mCCD(c1.1) cells. (A) Expression levels of *Slc22a17* mRNA by RT-PCR, in mCCD(c1.1) cells treated with 5 µg/mL lipopolysaccharides (LPS) for 12 h. *Slc22a17* mRNA expression was normalized to *Gapdh*. Data show means ± SEM of five experiments. Statistical analysis compares the effects of control versus LPS by unpaired *t*-test. (B) Expression of SLC22A17 in mCCD(c1.1) cells treated with 5 µg/mL LPS for 18 h was detected by immunofluorescence microscopy of permeabilized and non-permeabilized (“surface staining”) cells, using a SLC22A17 antibody directed against the extracellular N-terminus. Hoechst 33342 counterstains nuclei. Statistical analysis shows means ± SEM of 4–5 experiments and comparison of the two conditions by unpaired *t*-test. (C) Expression levels of *Lcn2* mRNA by RT-PCR in mCCD(c1.1) cells treated with LPS. *Lcn2* mRNA expression was normalized to *Gapdh*. Data show means ± SEM of six experiments. Statistical analysis compares the effects of control versus LPS by unpaired *t*-test. (D) Effect of LPS on expression of LCN2 protein in mCCD(c1.1) cells. Cellular LCN2 protein expression was normalized to β-actin. Data show means ± SEM of four experiments. Statistical analysis determines the effect of LPS on cellular LCN2 protein using unpaired *t*-test. (E) Effect of LPS on cellular expression and secretion of LCN2 protein in mCCD(c1.1) cell monolayers, grown to confluence on transwell filters. LPS or solvent were applied to both apical and basolateral chambers for 18 h. Cells were lysed, apical and basolateral media were collected and concentrated to the same volume, as described in the Methods. Corresponding corrected volumes of concentrated media were loaded for immunoblotting. Data show cellular LCN2 protein expression normalized to β-actin, as means ± SEM of 9–10 experiments. Statistical analysis determines the effect of LPS on cellular and apically or basolaterally secreted LCN2 protein, using one-way ANOVA. For a definition of asterisks, see “statistics” in the Methods.

### 2.5. ddAVP Posttranslationally Downregulates Unstimulated and LPS-Stimulated LCN2 in mCCD(c1.1) Cells

As shown in Figure 6A, LPS (5 µg/mL for 18 h) significantly reduced unstimulated and ddAVP-induced *Aqp2* mRNA expression in mCCD(c1.1) cells, thus confirming previous studies in mpkCCDc14 cells [35]. Despite LPS stimulation of *Lcn2* mRNA levels (Figure 6B), ddAVP (10 nM) had no effect on *Lcn2* mRNA as determined by RT-PCR and confirmed by qPCR (Figure 6C). In addition,

the CREB inhibitor 666-15 was ineffective (Figure 6C). Quite surprisingly, and in contrast to the mRNA data, both unstimulated and LPS-stimulated LCN2 protein expression and secretion were reduced by ddAVP (Figure 6D), suggesting a posttranslational effect of ddAVP on LCN2 expression and secretion. Indeed, co-application of cycloheximide (0.01 µg/mL for 3–6 h), a blocker of translational elongation [39], prevented the downregulation of LCN2 protein expression induced by ddAVP (Figure 6E), which indicates that ddAVP promotes LCN2 degradation following protein translation.

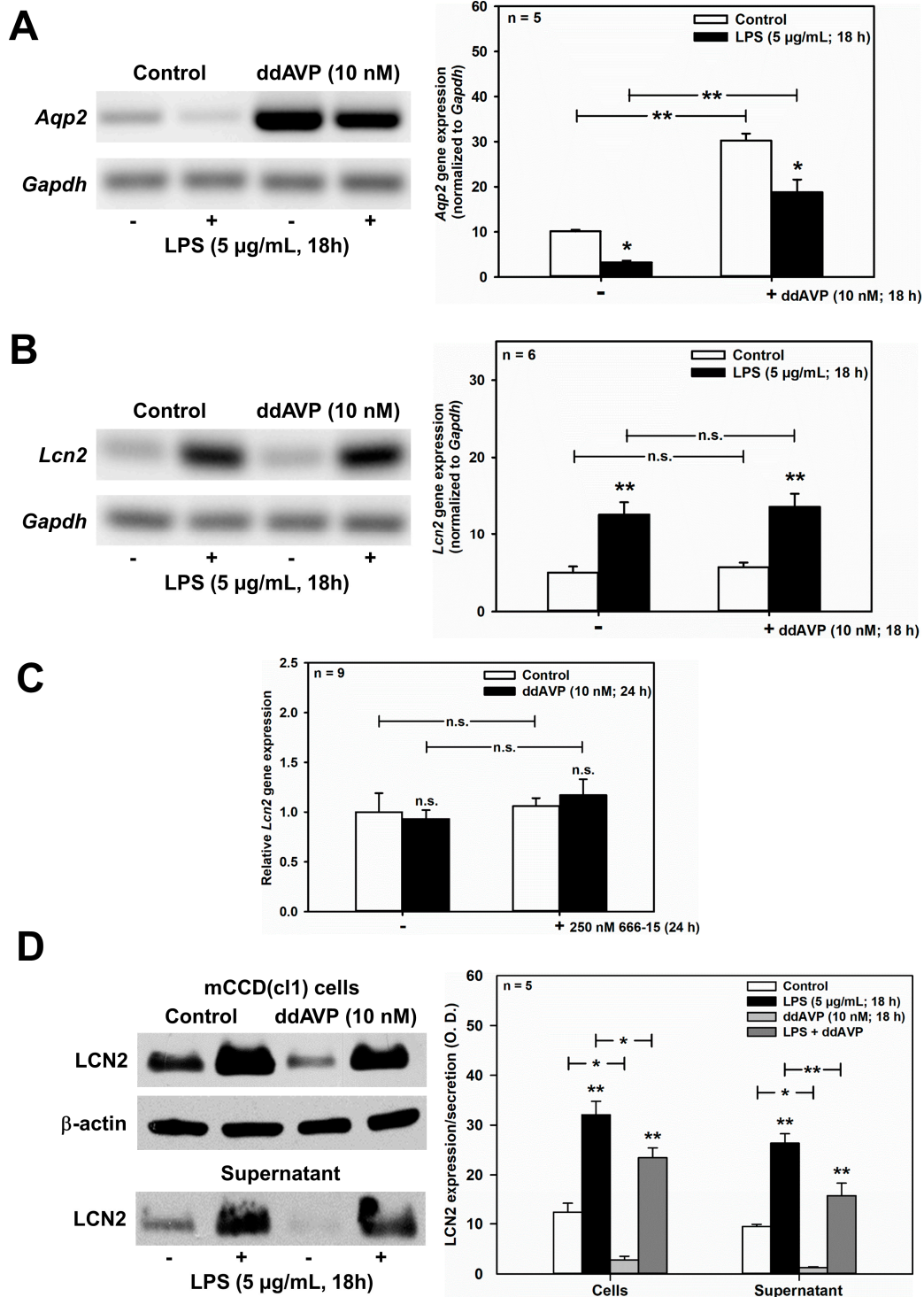
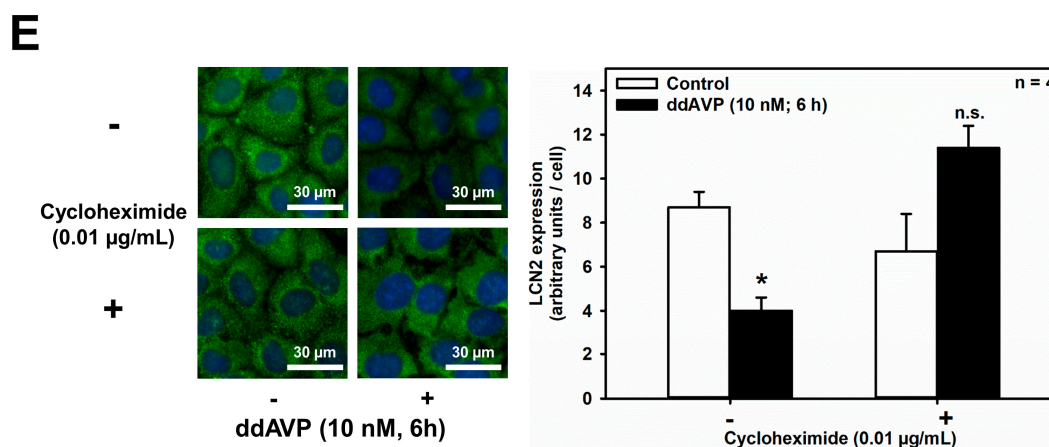


Figure 6. Cont.



**Figure 6.** ddAVP decreases *Lcn2*/LCN2 expression through a CREB-independent, posttranslational mode of action in mCCD(cl.1) cells. (A,B) Expression levels of *Aqp2* (A) and *Lcn2* (B) mRNA by RT-PCR in mCCD(cl.1) cells treated with ddAVP  $\pm$  LPS. Data are means  $\pm$  SEM of 5–6 experiments. Statistical analysis compares the expression levels of *Aqp2* or *Lcn2* in controls and ddAVP-treated cells  $\pm$  LPS, by one-way ANOVA. n.s. = not significant. (C) Expression levels of *Lcn2* mRNA by qPCR in mCCD(cl.1) cells treated with ddAVP  $\pm$  666-15. Data are means  $\pm$  SEM of nine experiments. Statistical analysis compares relative expression levels of *Lcn2* in controls and ddAVP-treated cells  $\pm$  666-15, by one-way ANOVA. n.s. = not significant. (D) Expression and secretion of LCN2 in mCCD(cl.1) cells treated with LPS, in the absence or presence of ddAVP. Media (supernatant), treated as described in Figure 5E, were immunoblotted. Cellular LCN2 protein expression was normalized to  $\beta$ -actin. Data are means  $\pm$  SEM of five experiments. Statistical analysis compares expression levels of cellular and secreted LCN2 in controls and ddAVP-treated cells  $\pm$  LPS, by one-way ANOVA. (E) Expression of LCN2 in mCCD(cl.1) cells treated with ddAVP for 6 h  $\pm$  cycloheximide, a blocker of translational elongation, was detected by immunofluorescence microscopy of permeabilized cells. Hoechst 33342 counterstains nuclei. Statistical analysis shows means  $\pm$  SEM of four experiments and comparison of the conditions  $\pm$  ddAVP by unpaired *t*-test. n.s. = not significant. For a definition of asterisks, see “statistics” in the Methods.

### 3. Discussion

It is interesting to note that SLC22A17 regulation is analogous to that of AQP2 in vivo and mpkCCDcl4 cells (reviewed in [3,10]). AVP stimulation of PKA activity increases abundance of *Aqp2*. PKA, in turn, activates *Aqp2* gene transcription, in part via increased CREB binding to cis elements of the *Aqp2* promoter. After longer periods of hypertonic challenge, NFAT5 also participates in increasing *Aqp2* gene transcription. In contrast, bacterial infection has been shown to interfere with *Aqp2* mRNA and AQP2 protein expression, via activation of the inflammatory pathway, involving NF- $\kappa$ B in vivo [40], and using LPS in cultured renal CCD mpkCCDcl4 [35]. Similarly, in mCCD(cl.1) cells, hyperosmolarity (Figure 1) and ddAVP (Figure 4A,B), respectively, increased SLC22A17 in an NFAT5- (Figure 3A,B) and CREB-dependent manner (Figure 4A,B), whereas LPS also reduced SLC22A17 expression (Figure 5A,B). The latter observation is similar to that of our previous study with mIMCD<sub>3</sub> cells, where LPS reduced SLC22A17 expression as well [20], most likely via NF- $\kappa$ B activation [36].

In our previous study, mIMCD<sub>3</sub> cells activated Wnt/TCF1/ $\beta$ -catenin signaling with inhibitory phosphorylation of GSK-3 $\beta$ , which caused SLC22A17 upregulation, in response to hyperosmolarity [20]. In silico analysis [41,42] indicated a putative TCF1 binding site 111 bases upstream of the *Slc22a17* gene, supporting the hypothesis that SLC22A17 is a downstream target of Wnt/ $\beta$ -catenin signaling. Is Wnt signaling linked to the central osmotic response pathway involving NFAT5? A study in HEK293 and mIMCD<sub>3</sub> cells indicated that inhibitory phosphorylation of GSK-3 $\beta$  contributes to high NaCl-induced activation of NFAT5, and suggested upstream regulation of NFAT5 by Wnt/GSK-3 $\beta$  signaling [43]. Supporting this, a putative *Nfat5* DNA consensus motif (osmotic response element (ORE), or tonicity-responsive enhancer (TonE)) [44], was identified in the human *SLC22A17* promoter

sequence ENSR00001455985/14:23820951-23822367 (<sup>828</sup>AGGAAAATGCCA<sup>839</sup>), which is compatible with the data obtained in Figure 3A,B. It would be worthwhile to test this putative ORE in future experiments, by site-directed mutagenesis of the sequence in a *Slc22a17* luciferase-reporter gene assay. Moreover, a search of the *Slc22a17* promoter sequence for CREB binding sites, with the tools JASPAR and PROMO [41,45], up to 2.7 kb upstream of the start codon, yielded a putative binding site at position -736 (Ralf Zarbock and Frank Thévenod, unpublished), supporting the results obtained in Figure 4.

The human *LCN2* gene (Ensembl ENSG00000148346; GenBank: X99133.1; 5869 bp) has ten putative regulatory promoter sequences. Similarly, as described for *Slc22a17*, we have also identified a putative NFAT5 DNA binding sequence in a region of the human *LCN2* gene (<sup>841</sup>TGGAAAAGGCT<sup>852</sup>), which could explain the *Lcn2* downregulation by hyperosmolarity in Figure 3C,D. In contrast, ddAVP did not influence *Lcn2* gene expression (Figure 6B,C). Rather, ddAVP reduced *LCN2* protein expression by a posttranslational mechanism (Figure 6D,E).

It is interesting to note that NFAT5 regulates *LCN2* and its receptor *SLC22A17* in an inverse manner, namely by causing upregulation of the receptor and downregulation of the ligand. In mIMCD<sub>3</sub> cells, hyperosmolarity induced an identical inverse regulation, via Wnt/ $\beta$ -catenin signaling [20], possibly because NFAT5 is downstream of Wnt/GSK-3 $\beta$  signaling [43] (see above). In addition, the oncogene BCR-ABL activated the JAK/STAT pathway in murine myeloblast-like cells, which increased *LCN2*, and repressed *SLC22A17* expression in a Ras and Runx1-dependent manner [13,46]. Hence, several signaling pathways exist to inversely control *LCN2* and its receptor, with different putative biological significance and outcomes (see below and [20] for a discussion).

Unexpectedly, the inverse regulation of *Slc22a17* and *Lcn2* at the gene level did not extend to ddAVP-mediated CREB regulation. Whereas CREB activation increased *Slc22a17*, ddAVP seemed to control *LCN2* via a posttranslational mechanism. For *Aqp2*, AVP not only regulates its expression at the gene level via CREB, but also PKA-dependent phosphorylation of the protein triggers its increased proteasomal and lysosomal degradation in a negative feedback loop [47]. This is unlikely for *LCN2*, because PKA does not phosphorylate the protein in vitro [48].

What could be the physiological significance of *SLC22A17* upregulation in the context of hyperosmotic stress and AVP-mediated urinary concentration? *SLC22A17* mediates receptor-mediated protein endocytosis in the distal nephron [14]. Endocytosed proteins are trafficked to lysosomes [14], where they are degraded. We speculate that *SLC22A17* promotes osmotolerance by feeding cells with amino acids as precursors/osmolytes, to maintain iso-osmolarity with the interstitium. However, this will require experimental proof. Downregulation of *LCN2* in the same context would also foster cellular protection during hyperosmotic stress. It has been proposed that *LCN2* upholds epithelial growth and proliferation (reviewed in [49]), which is associated with increased DNA replication and transcription. Osmotic stress induces DNA strand breaks, inhibits DNA repair and increases oxidative stress, which may all lead to increased mutation rates in dividing cells, unless proliferation is inhibited, allowing for efficient repair.

## 4. Materials and Methods

### 4.1. Materials

Lipopolysaccharides (LPS) from *Escherichia coli* (cat. # L3129), [deamino-Cys1, D-Arg8]-vasopressin acetate salt hydrate (ddAVP, desmopressin) cat. # V1005) and protease inhibitor cocktail (cat. # P8340) were obtained from Sigma–Aldrich (Taufkirchen, Germany). The 3-(3-Aminopropoxy)-N-[2-[[3-[[[4-chloro-2-hydroxyphenyl] amino]carbonyl]-2-naphthalenyl] oxy] ethyl]-2-naphthalenecarboxamide hydrochloride (666-15) (cat. # 5661) was obtained from Tocris Bioscience. Cycloheximide (cat. # ALX-380-269-G001) was obtained from Enzo Life Sciences (Lörrach, Germany). All other reagents were of the highest purity grade possible. Materials were dissolved in water, ethanol, or dimethyl sulfoxide (DMSO). In control experiments, solvents were added to cells at concentrations not exceeding 0.2%. Antibodies are listed in Table 1.

**Table 1.** Primary antibodies.

Immunogen	Host Species	Manufacturer	Catalog #	Application	Dilution
Rat LCN2	goat	RD Biosystems	AF3508	IB *	1:200–1:300
Mouse LCN2	rabbit	Abcam	Ab63929	IF *	1:250–1:1000
Rat SLC22A17 (C-terminus)	rabbit	[14]	Ig-1086	IB	1:100–1:2000
Rat SLC22A17 (N-terminus)	rabbit	[14]	Ig-1095	IF	1:100–1:1000
Human b-actin	mouse	[14]	A5316	IB	1:20,000
Human GAPDH (14C10)	mouse	Sigma-Aldrich	2118	IB	1:20,000
Human Na <sup>+</sup> ,K <sup>+</sup> - ATPase $\alpha$ 1-subunit	rabbit	Cell Signaling	30105	IB	1:250–1:500
Human Lamin A/C (4C11)	mouse	Cell Signaling	4777	IB	1:20,000
Human NFAT5	rabbit	[24]	N/A	IB	1:6000
Human I $\kappa$ B-a	rabbit	Santa Cruz	Sc-371	IB	1:1000

\* IB = immunoblotting; \* IF = immunofluorescence.

## 4.2. Methods

### 4.2.1. Culture of mCCD(cl.1) Cells

The mouse (m)CCD(cl.1) cell line [50] was obtained from Dr. Edith Hummler (University of Lausanne, CH). Cells (passage 25–34) were cultured in Dulbecco's modified Eagle's medium (DMEM)/nutrient mixture F-12 (1:1) (Gibco cat. # 31330), supplemented with 2.5 mM L-glutamine, 15 mM Hepes, 5% fetal bovine serum (FBS), 100 U/mL penicillin, and 100  $\mu$ g/mL streptomycin, 0.9  $\mu$ M insulin (Sigma–Aldrich; cat. # I1882), 5  $\mu$ g/mL apo-transferrin (Sigma–Aldrich; cat. # T2252), 10 ng/mL EGF (Sigma–Aldrich; cat. # E9644), 1 nM T3 (Sigma–Aldrich; cat. # T6397), and 50 nM dexamethasone (Sigma–Aldrich; cat. # D4902) [51]. Cells were cultured in 25 cm<sup>2</sup> standard tissue culture flasks (Sarstedt, Nümbrecht, Germany) at 37 °C in a humidified incubator with 5% CO<sub>2</sub>, and passaging was performed twice a week upon reaching 90% confluence. Inhibitors (666-15, cycloheximide) were preincubated for 60 min.

### 4.2.2. Osmolarity/Tonicity Experiments

Osmolarity is the measure of solute concentration per unit volume of solvent. Tonicity is the measure of the osmotic pressure gradient between two solutions across biological membranes. Unlike osmolarity, tonicity is only influenced by solutes that cannot cross this semipermeable membrane, because they create and influence the osmotic pressure gradient between the intracellular and extracellular compartments. Unless otherwise indicated, in osmolarity/tonicity experiments, cell lines were cultured for 24 h in a standard culture medium (=300 mosmol/L) after seeding. Then the medium was replaced with either normosmotic standard culture medium or hyperosmotic medium of 400–500 mosmol/L (by addition of 50 mmol/L NaCl from 3 M stock solutions), and cultured for up to 72 h (CCD are physiologically exposed to comparable hyperosmotic interstitial concentrations of NaCl [7,8]). NaCl initially does not cross the cell membrane, and therefore exerts an osmotic pressure gradient on the cells (hypertonicity). For simplification, the term “osmolarity” henceforth refers to osmolarity and tonicity.

### 4.2.3. Transient Transfection

Cells were transiently transfected with *Nfat5* siRNA (sense primers for Stealth siRNA (Invitrogen, San Diego, CA, USA) 5'-GGUGUUGCAGGUAUUUGUGGGCAAU-3',

5'-GGAUUCUAUCAGGCCUGUAGAGUAA-3', 5'-CCUAGUUCUCAAGAUCAGCAAGUAA-3' [24]) or siRNA duplex negative control (Eurogentec cat. # SR-CL000-005). For lipid-based transfections,  $1.0 \times 10^5$  mCCD(c1.1) cells were seeded in 6-well plates and transfected 24 h later at ~40% confluence with 5 nM siRNA, using Lipofectamine RNAiMAX (Thermo Fisher Scientific, Schwerte, Germany), according to the manufacturer's instructions. After 24 h, the medium was exchanged to 300 or 400 mosmol/L media.

Transfection by electroporation was performed as described previously [52], with slight modifications. In brief,  $2.0 \times 10^6$  mCCD(c1.1) cells were electroporated at 300 mV and 960  $\mu$ F, using a Bio-Rad Gene Pulser, and transfected with 100–250 nM siRNA. For osmolarity experiments,  $1 \times 10^6$  electroporated cells were seeded in 25 cm<sup>2</sup> flasks, or  $2 \times 10^4$  cells seeded on glass cover slips.

#### 4.2.4. RNA Extraction, cDNA Synthesis and Reverse Transcription PCR (RT-PCR)

Isolation of total RNA, synthesis of cDNA and PCR reactions were performed as previously described [20,53]. PCR reactions were performed using specific primers and cycling protocols (Table 2). Gel documentation and densitometry analysis were performed using Image Lab Software version 5.2 (Bio-Rad Laboratories), with correction for loading by the housekeeping gene glyceraldehyde-3-phosphate dehydrogenase (*Gapdh*).

**Table 2.** Protocols for reverse transcription PCR.

	<i>Gapdh</i>	<i>Aqp2</i>	<i>Lcn2</i>	<i>Slc22a17</i>
<b>Accession number</b>	NM_001289726.1	NM_009699.3	NM_008491.1	NM_021551.4
<b>Forward primer (5'-3')</b>	AGGGCTCA TGACCACAGT	TGGCTGTCAA TGCTCTCCAC	CCACCACGGA CTACAACCAG	CAGCCACCTCCT AACCGCTGTG
<b>Reverse primer (5'-3')</b>	TGCAGGGATG ATGTTCTG	GGAGCAGCCG GTGAAATAGA	AGCTCCTTGG TTCTTCCATACA	CTCCCACTAGGCT CAAAGGCTGTCT
<b>Reference</b>	NCBI Primer-BLAST	[53]	[39]	[39]
<b>Activation</b>	5 min 95 °C	5 min 95 °C	5 min 95 °C	5 min 95 °C
<b>Cycle number</b>	18–22	31–33	20–25	27–29
<b>Denaturation</b>	30 s 94 °C	30 s 94 °C	30 s 94 °C	30 s 94 °C
<b>Annealing</b>	30 s 60 °C	30 s 62 °C	30 s 60 °C	30 s 60 °C
<b>Extension</b>	30 s 72 °C	30 s 72 °C	30 s 72 °C	30 s 72 °C
<b>Final Extension</b>	7 min 72 °C	7 min 72 °C	7 min 72 °C	7 min 72 °C
<b>PCR product (bp)</b>	112	200	100	86

#### 4.2.5. Quantitative PCR (qPCR)

RNA extraction and cDNA synthesis were performed as described for the RT-PCR protocol. Primers were designed using PrimerBLAST software (NCBI) and/or taken from the literature. The primers were obtained from Eurofins Genomics (Table 3) and tested for primer efficiency using serially diluted cDNA (see Table 3). Quantitative PCR (qPCR) was performed essentially as described [20,54] in a StepOnePlus Real-Time PCR System (Applied Biosystems), using KAPA SYBR FAST qPCR Master Mix Universal and High ROX Reference Dye (Roche). The cycling conditions were activation at 95 °C for 5 min, followed by 40 cycles (42 cycles for *Aqp2*) of 95 °C for 3 s, and of 60 °C (62 °C for *Aqp2*) for 30 s, with melt curve analysis to check amplification specificity. Gene expression levels were calculated according to the  $2^{-\Delta C_q}$  method relative to the sample with the highest expression (minimum C<sub>q</sub>) [55]. The data obtained were normalized to the expression of two stable reference genes: *Gapdh* and  $\beta$ -actin (*Actb*).

**Table 3.** qPCR primers.

Gene-Name (Accession Number)	Forward (5'-3')	Reverse (5'-3')	Reference	Amplicon Size (bp)	Efficiency(%)
<i>Actb</i> (NM_007393.5)	CGTGCGTGAC ATCAAAGAGAA	GGCCATCTC CTGCTCGAA	[20]	102	102
<i>Gapdh</i> (NM_001289726.1)	CGGCCGCAT CTTCTTG TG	CCGACCTTCA CCATTTTGCTAC	[20]	100	100
<i>Lcn2</i> (NM_008491.1)	CCACCACGG ACTACAACCAG	AGTCCTTGGT TCTTCCATACA	[20]	98	98
<i>Slc22a17</i> (NM_021551.4)	CAGCCACCTC CTAACCGCTGTG	CTCCCACTAGGC TCAAAGGCTGCT	[20]	110	110
<i>Aqp2</i> (NM_009699.3)	TGGCTGTCAA TGCTCTCCAC	GGAGCAGCCG GTGAAATAGA	[53]	92	92

#### 4.2.6. Measurements of Transepithelial Electrical Resistance (TEER) of Cell Monolayers

Cells ( $2 \times 10^4$ ) were plated in transwell filters for 24-well plates with 0.4- $\mu\text{m}$  pore size and 0.33-cm<sup>2</sup> surface area (cat. # 3470, Costar Transwell-Clear, Corning, Wiesbaden, Germany). After two days, transepithelial electrical resistance (TEER) was measured daily, using an epithelial volt-ohm meter EVOM with an STX2 electrode (World Precision Instruments, Friedberg, Germany), at room temperature. Reported resistance readings were corrected for background by subtracting the resistance of empty cell-free inserts in culture medium of  $140.3 \pm 4.0 \Omega$  (means  $\pm$  SEM;  $n = 17$ ). Treatments were started 14–15 days after seeding, when TEER reached a stable value of  $284.3 \pm 15.9 \Omega \times \text{cm}^2$  (means  $\pm$  SEM;  $n = 17$ ). LPS and/or ddAVP were then added to both the apical (upper chamber, 300  $\mu\text{L}$  medium) and basolateral (lower chamber, 1000  $\mu\text{L}$  medium) compartments and incubated for 18 h at 37 °C, prior to measurements of *Lcn2* expression and secretion.

#### 4.2.7. Determination of LCN2 Expression and Secretion

LCN2 secretion by mCCD(cl.1) cells was detected by immunoblotting. Media from the apical and basolateral compartments of transwell filters were concentrated at room temperature to a final volume of 100–150  $\mu\text{L}$ , using Vivaspin 500 centrifugal concentrators (10 kDa molecular weight cut-off; cat. # VS0102, Sartorius), corrected for volume differences and used for immunoblotting. To determine cellular LCN2 expression, cells grown on filters were lysed in 30  $\mu\text{L}$ /well of lysis buffer (25 mM Tris pH 7.4, 2 mM Na<sub>3</sub>VO<sub>4</sub>, 10 mM NaF, 10 mM Na<sub>4</sub>P<sub>2</sub>O<sub>7</sub>, 1 mM ethylenediaminetetraacetic acid (EDTA), 1 mM ethylene glycol-bis( $\beta$ -aminoethyl ether)-N,N,N',N'-tetraacetic acid (EGTA), 1% Nonidet P-40) containing protease inhibitors. For *Lcn2* expression by RT-PCR, cells grown on transwell filters were washed once with phosphate buffered saline (PBS), and collected by scraping in 100  $\mu\text{L}$  PBS, using a rubber policeman.

#### 4.2.8. Isolation of Plasma Membrane Enriched Microsomes

An amount of  $2 \times 10^6$  mCCD(cl.1) cells were seeded into 175 cm<sup>2</sup> culture flasks and grown for 24 h in standard culture medium before osmotic challenge for 72 h. Plasma membranes were obtained by differential ultracentrifugation at 4 °C. Cells were homogenized by nitrogen pressure cavitation in a Parr Instruments 45 mL cell disruption vessel (Moline, IL, USA) for 2 min at 1000 p.s.i. To remove unbroken cells, nuclei, large debris and mitochondria, homogenate was centrifuged at 8000 $\times g$  for 20 min, and the resulting supernatant was centrifuged for 45 min at 35,000 $\times g$ , to yield a microsomal fraction in the pellet, before being resuspended and supplemented with protease inhibitors. Plasma membrane purity was verified by immunoblotting and showed about a 10-fold enrichment of Na<sup>+</sup>,K<sup>+</sup>-ATPase (Figure 1C).

#### 4.2.9. Isolation of Nuclei

An amount of  $4 \times 10^5$  cells were plated into 75 cm<sup>2</sup> culture flasks and grown for 48 h, to reach a confluency of ~80%, before medium was replaced by 300–500 mosmol/L media and incubated for an additional 24 h. Nuclei and post-nuclear supernatant were separated as reported elsewhere [56]. All steps were performed at 4 °C. Cells were swelled in hypotonic buffer A (10 mM HEPES-KOH, pH 7.9, 1.5 mM MgCl<sub>2</sub>, 10 mM KCl, 0.5 mM dithiothreitol (DTT), 0.05% Nonidet P-40) containing protease inhibitors, Tenbroeck homogenized, and nuclei were pelleted (220× g, 5 min). Nuclei were washed with buffer A + 0.3% Nonidet P-40, to remove cytoplasmic contaminants, and pelleted (600× g, 5 min). Nuclei were resuspended in 0.25 M sucrose/10 mM MgCl<sub>2</sub>, layered over 0.35 M sucrose/0.5 mM MgCl<sub>2</sub> and centrifuged at 1430× g for 5 min. Purified nuclei were stored in buffer B (20 mM HEPES-KOH, pH 7.9, 25% glycerol, 420 mM NaCl, 1.5 mM MgCl<sub>2</sub>, 0.2 mM EDTA, 0.5 mM DTT, 0.05% Nonidet P-40), containing protease inhibitors. Samples were sonicated using a Branson Digital Sonifier (Danbury, CT, USA) (3 × 5 s at 20% output) prior to protein determination by the Bradford method [57], using bovine serum albumin (BSA) as a standard.

#### 4.2.10. Immunoblotting

Sodium dodecyl sulfate polyacrylamide gel electrophoresis (SDS-PAGE) and immunoblotting were essentially performed according to standard procedures of wet transfer, as described earlier [14], with the exception of LCN2 immunoblots, which were electroblotted by rapid semi-dry transfer (Bio-Rad Laboratories Trans-Blot Turbo). Cells were washed in PBS, scraped and homogenized by sonication in an isosmotic sucrose buffer. Protein concentration was determined by the Bradford method [57]. Equal amounts of protein (5–30 µg) were subjected to SDS-PAGE and immunoblotted. Primary antibodies and their dilutions are listed in Table 1. Horseradish peroxidase-conjugated secondary antibodies were purchased from Santa Cruz Biotechnology, Inc. or GE Healthcare (Heidelberg, Germany or Schwerte, Germany) and used at 1:2500–1:30,000 dilutions. Densitometry analysis was performed using ImageJ software (<https://imagej.net/>) [58].

#### 4.2.11. Immunofluorescence Staining and Microscopy

mCCD(cl.1) cells ( $0.5\text{--}2.0 \times 10^4$  cells / well) were plated on glass coverslips and cultured for 24–72 h, to reach a confluence of 40%–50% prior to treatments.

For surface staining (at 4 °C), cells were blocked with 1% BSA-PBS for 1 h, followed by incubation with a rabbit polyclonal IgG antibody against the N-terminus of rodent anti-SLC22A17 (1:100 dilution in 1% BSA-PBS = 10 µg/mL) for 2 h. Cells were then incubated with secondary Alexa Fluor 488-conjugated goat anti-rabbit IgG (1:600; cat. # A-11008, Thermo Fisher) for 1 h, and fixed with 4% paraformaldehyde (PFA) in PBS for 30 min at room temperature. Nuclei were counterstained with 0.8 µg/mL Hoechst 33342 for 5 min. Coverslips were embedded with DAKO fluorescent mounting medium, and images were acquired as described elsewhere [59].

For total cellular SLC22A17 staining at room temperature (LPS experiments), cells were fixed with 4% PFA in PBS for 30 min, permeabilized with 1% SDS in PBS for 15 min, and blocked with 1%–2% BSA-PBS for 30–40 min. N-terminal rodent anti-SLC22A17 (1:100–1000 dilution in 1% BSA-PBS) or LCN2 polyclonal rabbit IgG (Abcam Ab63929: 1:250–1000 dilution in 2% BSA-PBS) were incubated for 2 h. Subsequent steps were identical to surface staining procedures. For quantitative determination of Alexa Fluor 488-conjugated SLC22A17 or LCN2 in mCCD(cl.1) cells, 200 to 500 cells, in six to twelve microscopic fields, were analyzed for each experiment with the MetaMorph software (ICIT, Frankfurt am Main, Germany) [59].

#### 4.2.12. Statistics

Unless otherwise indicated, the experiments were repeated at least three times with independent cultures. Means ± SEM are shown. Statistical analysis, using unpaired Student's *t*-test, was carried

out with GraphPad Prism v. 5.01 (GraphPad Software Inc., San Diego, CA, USA). For more than two groups, one-way ANOVA with Tukey or Dunnett's *post-hoc* test, assuming equality of variance, was applied. Results with  $p < 0.05$  were considered statistically significant. The dose–response curve of the effect of LPS on LCN2 secretion was fitted with the Sigma Plot 12.5 spreadsheet program, assuming a sigmoidal function and using the Hill equation. Significance levels were labelled in the Figures as follows: \* =  $p < 0.05$ ; \*\* =  $p < 0.01$ ; \*\*\* =  $p < 0.001$ .

## 5. Conclusions

In summary (see Figure 7), the present study unveils a signaling mechanism in the cultured CCD cell line mCCD(cl.1) involved in the regulation of the expression of the LCN2 receptor SLC22A17, by hyperosmolarity via NFAT5, and by AVP via CREB, which parallels *Aqp2* regulation, suggesting SLC22A17 plays a role in adaptation to osmotic stress. In contrast, the ligand of SLC22A17, LCN2 is downregulated by hyperosmolarity and AVP in a NFAT5-dependent, CREB-independent manner. Rather, PKA-dependent posttranslational control of LCN2 occurs via ill-defined mechanisms. We speculate that LCN2 downregulation may prevent the increased proliferation and permanent damage of osmotically stressed cells.

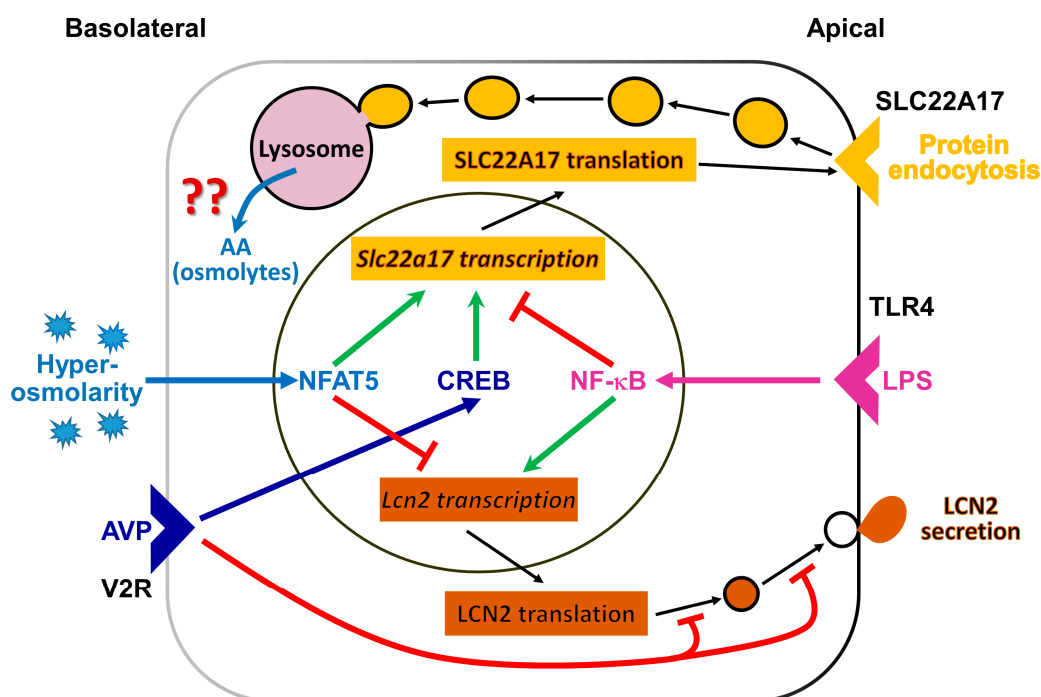


**Figure 7.** Regulation of lipocalin-2 receptor (SLC22A17) and lipocalin 2 (LCN2) abundance in the renal cortical collecting duct cell line mCCD(cl.1). Several extracellular stimuli control SLC22A17 and LCN2 abundance, by acting on *Slc22a17* and *Lcn2* gene transcription or posttranslational *Lcn2* expression. Shown are pathways mediated by arginine vasopressin (AVP), binding to the arginine vasopressin receptor-2 (V2R) (dark blue), hyperosmolarity/tonicity (light blue) and/or inflammation (magenta). AVP stimulation (dark blue arrow) results from adenylyl cyclase activation, increased intracellular cAMP concentration, and protein kinase A (PKA) activation. PKA, in turn, increases cAMP-responsive element binding protein (CREB) activity. NF-κB activation (magenta arrow) occurs by inflammatory stimuli, such as lipopolysaccharide (LPS) via toll-like receptor 4 (TLR4). After longer periods of hypertonic challenge, the nuclear factor of activated T-cells 5 (NFAT5; also known as TonEBP or OREBP) is activated. Apically expressed SLC22A17 promotes protein endocytosis, possibly to provide amino acids (AA) and/or osmolytes for osmotolerance, but this remains unproven. Cells secrete LCN2 to combat bacterial infections and/or promote proliferation after epithelial damage. ↑ (green) = stimulation; ↓ (red) = inhibition. For further details, see text.

**Supplementary Materials:** Supplementary materials can be found at <http://www.mdpi.com/1422-0067/20/21/5398/s1>.

**Author Contributions:** Conceptualization, F.T.; Formal analysis, S.P., B.S., R.M. and F.T.; Funding acquisition, F.T.; Investigation, W.-K.L. and F.T.; Methodology, S.P., R.M., and B.S.; Project administration, B.S. and F.T.; Supervision, W.-K.L. and F.T.; Validation, W.-K.L. and F.T.; Visualization, S.P. and F.T.; Writing—original draft, F.T.; Writing—review and editing, S.P., B.S., R.M., W.-K.L., and F.T.

**Acknowledgments:** This work was supported by the Deutsche Forschungsgemeinschaft (DFG TH345/11-1), a BMBF grant between Germany and Mexico (BMBF 01DN16039), an ERASMUS+ Student Mobility Traineeship, and the Centre for Biomedical Training and Research (ZBAF) of the University of Witten/Herdecke. The authors are grateful to Drs. Hyug Moo Kwon (Ulsan National Institute of Science and Technology, School of Nano-Bioscience and Chemical Engineering, Ulsan, South Korea) and Eric Feraille (University of Geneva, Department of Cellular Physiology and Metabolism, Geneva, Switzerland) for granting permission to use their *Nfat5* plasmids, antibodies and siRNAs. The authors thank Dr. Johannes Fels (Physiology, Witten/Herdecke University) for his valuable discussions.

**Conflicts of Interest:** The authors declare that they have no conflict of interest. The data sets used and/or analyzed in the current study are available from the corresponding authors upon reasonable request.

## References

1. Knepper, M.A.; Hoffert, J.D.; Packer, R.K.; Fenton, R.A. Urine Concentration and Dilution. In *Brenner & Rector's The Kidney*, 8th ed.; Brenner, B.M., Ed.; Saunders: Philadelphia, PA, USA, 2008; Volume 1, pp. 308–329.
2. Brown, D.; Nielsen, S. Cell Biology of Vasopressin Action. In *Brenner & Rector's The Kidney*, 8th ed.; Brenner, B.M., Ed.; Saunders: Philadelphia, PA, USA, 2008; Volume 1.
3. Hasler, U.; Leroy, V.; Martin, P.Y.; Feraille, E. Aquaporin-2 abundance in the renal collecting duct: New insights from cultured cell models. *Am. J. Physiol. Renal Physiol.* **2009**, *297*, F10–F18. [[CrossRef](#)] [[PubMed](#)]
4. Hozawa, S.; Holtzman, E.J.; Ausiello, D.A. cAMP motifs regulating transcription in the aquaporin 2 gene. *Am. J. Physiol.* **1996**, *270*, C1695–C1702. [[CrossRef](#)] [[PubMed](#)]
5. Matsumura, Y.; Uchida, S.; Rai, T.; Sasaki, S.; Marumo, F. Transcriptional regulation of aquaporin-2 water channel gene by cAMP. *J. Am. Soc. Nephrol.* **1997**, *8*, 861–867. [[PubMed](#)]
6. Yasui, M.; Zelenin, S.M.; Celsi, G.; Aperia, A. Adenylate cyclase-coupled vasopressin receptor activates AQP2 promoter via a dual effect on CRE and AP1 elements. *Am. J. Physiol.* **1997**, *272*, F443–F450. [[CrossRef](#)] [[PubMed](#)]
7. Ullrich, K.J.; Drenckhahn, F.O.; Jarausch, K.H. Studies on the problem of urine concentration and dilution; osmotic behavior of renal cells and accompanying electrolyte accumulation in renal tissue in various diuretic conditions. *Pflug. Arch. Gesamte Physiol. Menschen Tiere* **1955**, *261*, 62–77. [[CrossRef](#)] [[PubMed](#)]
8. Jarausch, K.H.; Ullrich, K.J. Studies on the problem of urine concentration and dilution; distribution of electrolytes (sodium, potassium, calcium, magnesium, anorganic phosphate), urea amino acids and exogenous creatinine in the cortex and medulla of dog kidney in various diuretic conditions. *Pflug. Arch. Gesamte Physiol. Menschen Tiere* **1956**, *262*, 537–550.
9. Burg, M.B.; Ferraris, J.D.; Dmitrieva, N.I. Cellular response to hyperosmotic stresses. *Physiol. Rev.* **2007**, *87*, 1441–1474. [[CrossRef](#)]
10. Hasler, U. Controlled aquaporin-2 expression in the hypertonic environment. *Am. J. Physiol. Cell Physiol.* **2009**, *296*, C641–C653. [[CrossRef](#)]
11. Abergel, R.J.; Clifton, M.C.; Pizarro, J.C.; Warner, J.A.; Shuh, D.K.; Strong, R.K.; Raymond, K.N. The siderocalin/enterobactin interaction: A link between mammalian immunity and bacterial iron transport. *J. Am. Chem. Soc.* **2008**, *130*, 11524–11534. [[CrossRef](#)]
12. Paragas, N.; Kulkarni, R.; Werth, M.; Schmidt-Ott, K.M.; Forster, C.; Deng, R.; Zhang, Q.; Singer, E.; Klose, A.D.; Shen, T.H.; et al. Alpha-Intercalated cells defend the urinary system from bacterial infection. *J. Clin. Investig.* **2014**, *124*, 2963–2976. [[CrossRef](#)]
13. Devireddy, L.R.; Gazin, C.; Zhu, X.; Green, M.R. A cell-surface receptor for lipocalin 24p3 selectively mediates apoptosis and iron uptake. *Cell* **2005**, *123*, 1293–1305. [[CrossRef](#)] [[PubMed](#)]
14. Langelueddecke, C.; Roussa, E.; Fenton, R.A.; Wolff, N.A.; Lee, W.K.; Thévenod, F. Lipocalin-2 (24p3/neutrophil gelatinase-associated lipocalin (NGAL)) receptor is expressed in distal nephron and mediates protein endocytosis. *J. Biol. Chem.* **2012**, *287*, 159–169. [[CrossRef](#)] [[PubMed](#)]

15. Dizin, E.; Hasler, U.; Nlandu-Khodo, S.; Fila, M.; Roth, I.; Hernandez, T.; Doucet, A.; Martin, P.Y.; Feraille, E.; de Seigneux, S. Albuminuria induces a proinflammatory and profibrotic response in cortical collecting ducts via the 24p3 receptor. *Am. J. Physiol. Renal Physiol.* **2013**, *305*, F1053–F1063. [[CrossRef](#)] [[PubMed](#)]
16. Thévenod, F.; Wolff, N.A. Iron transport in the kidney: Implications for physiology and cadmium nephrotoxicity. *Met. Integr. Biometal Sci.* **2016**, *8*, 17–42. [[CrossRef](#)] [[PubMed](#)]
17. Thévenod, F.; Fels, J.; Lee, W.K.; Zarbock, R. Channels, transporters and receptors for cadmium and cadmium complexes in eukaryotic cells: Myths and facts. *Biometals* **2019**, *32*, 469–489. [[CrossRef](#)]
18. Christensen, E.I.; Birn, H. Megalin and cubilin: Multifunctional endocytic receptors. *Nat. Rev. Mol. Cell Biol.* **2002**, *3*, 256–266. [[CrossRef](#)]
19. Lee, J.W.; Chou, C.L.; Knepper, M.A. Deep Sequencing in Microdissected Renal Tubules Identifies Nephron Segment-Specific Transcriptomes. *J. Am. Soc. Nephrol.* **2015**, *26*, 2669–2677. [[CrossRef](#)]
20. Betten, R.; Scharner, B.; Probst, S.; Edemir, B.; Wolff, N.A.; Langelueddecke, C.; Lee, W.K.; Thévenod, F. Tonicity inversely modulates lipocalin-2 (Lcn2/24p3/NGAL) receptor (SLC22A17) and Lcn2 expression via Wnt/beta-catenin signaling in renal inner medullary collecting duct cells: Implications for cell fate and bacterial infection. *Cell Commun. Signal.* **2018**, *16*, 74. [[CrossRef](#)]
21. Cabedo Martinez, A.I.; Weinhaupl, K.; Lee, W.K.; Wolff, N.A.; Storch, B.; Zerko, S.; Konrat, R.; Kozminski, W.; Breuker, K.; Thévenod, F.; et al. Biochemical and Structural Characterization of the Interaction between the Siderocalin NGAL/LCN2 (Neutrophil Gelatinase-associated Lipocalin/Lipocalin 2) and the N-terminal Domain of Its Endocytic Receptor SLC22A17. *J. Biol. Chem.* **2016**, *291*, 2917–2930. [[CrossRef](#)]
22. Marples, D.; Christensen, B.M.; Frokiaer, J.; Knepper, M.A.; Nielsen, S. Dehydration reverses vasopressin antagonist-induced diuresis and aquaporin-2 downregulation in rats. *Am. J. Physiol.* **1998**, *275*, F400–F409. [[CrossRef](#)]
23. Preisser, L.; Teillet, L.; Aliotti, S.; Gobin, R.; Berthonaud, V.; Chevalier, J.; Corman, B.; Verbavatz, J.M. Downregulation of aquaporin-2 and -3 in aging kidney is independent of V<sub>2</sub> vasopressin receptor. *Am. J. Physiol. Renal Physiol.* **2000**, *279*, F144–F152. [[CrossRef](#)] [[PubMed](#)]
24. Hasler, U.; Jeon, U.S.; Kim, J.A.; Mordasini, D.; Kwon, H.M.; Feraille, E.; Martin, P.Y. Tonicity-responsive enhancer binding protein is an essential regulator of aquaporin-2 expression in renal collecting duct principal cells. *J. Am. Soc. Nephrol.* **2006**, *17*, 1521–1531. [[CrossRef](#)] [[PubMed](#)]
25. Sheen, M.R.; Kim, J.A.; Lim, S.W.; Jung, J.Y.; Han, K.H.; Jeon, U.S.; Park, S.H.; Kim, J.; Kwon, H.M. Interstitial tonicity controls TonEBP expression in the renal medulla. *Kidney Int.* **2009**, *75*, 518–525. [[CrossRef](#)] [[PubMed](#)]
26. Ko, B.C.; Turck, C.W.; Lee, K.W.; Yang, Y.; Chung, S.S. Purification, identification, and characterization of an osmotic response element binding protein. *Biochem. Biophys. Res. Commun.* **2000**, *270*, 52–61. [[CrossRef](#)]
27. Miyakawa, H.; Woo, S.K.; Dahl, S.C.; Handler, J.S.; Kwon, H.M. Tonicity-responsive enhancer binding protein, a rel-like protein that stimulates transcription in response to hypertonicity. *Proc. Natl. Acad. Sci. USA* **1999**, *96*, 2538–2542. [[CrossRef](#)]
28. DiGiovanni, S.R.; Nielsen, S.; Christensen, E.I.; Knepper, M.A. Regulation of collecting duct water channel expression by vasopressin in Brattleboro rat. *Proc. Natl. Acad. Sci. USA* **1994**, *91*, 8984–8988. [[CrossRef](#)]
29. Hayashi, M.; Sasaki, S.; Tsuganezawa, H.; Monkawa, T.; Kitajima, W.; Konishi, K.; Fushimi, K.; Marumo, F.; Saruta, T. Expression and distribution of aquaporin of collecting duct are regulated by vasopressin V<sub>2</sub> receptor in rat kidney. *J. Clin. Investig.* **1994**, *94*, 1778–1783. [[CrossRef](#)]
30. Hasler, U.; Mordasini, D.; Bens, M.; Bianchi, M.; Cluzeaud, F.; Rousselot, M.; Vandewalle, A.; Feraille, E.; Martin, P.Y. Long term regulation of aquaporin-2 expression in vasopressin-responsive renal collecting duct principal cells. *J. Biol. Chem.* **2002**, *277*, 10379–10386. [[CrossRef](#)]
31. Schenk, L.K.; Bolger, S.J.; Luginbuhl, K.; Gonzales, P.A.; Rinschen, M.M.; Yu, M.J.; Hoffert, J.D.; Pisitkun, T.; Knepper, M.A. Quantitative proteomics identifies vasopressin-responsive nuclear proteins in collecting duct cells. *J. Am. Soc. Nephrol.* **2012**, *23*, 1008–1018. [[CrossRef](#)]
32. Xie, F.; Li, B.X.; Kassenbrock, A.; Xue, C.; Wang, X.; Qian, D.Z.; Sears, R.C.; Xiao, X. Identification of a Potent Inhibitor of CREB-Mediated Gene Transcription with Efficacious in Vivo Anticancer Activity. *J. Med. Chem.* **2015**, *58*, 5075–5087. [[CrossRef](#)]
33. Takeuchi, O.; Hoshino, K.; Kawai, T.; Sanjo, H.; Takada, H.; Ogawa, T.; Takeda, K.; Akira, S. Differential roles of TLR2 and TLR4 in recognition of gram-negative and gram-positive bacterial cell wall components. *Immunity* **1999**, *11*, 443–451. [[CrossRef](#)]

34. Wolfs, T.G.; Buurman, W.A.; van Schadewijk, A.; de Vries, B.; Daemen, M.A.; Hiemstra, P.S.; van 't Veer, C. In vivo expression of Toll-like receptor 2 and 4 by renal epithelial cells: IFN-gamma and TNF-alpha mediated up-regulation during inflammation. *J. Immunol.* **2002**, *168*, 1286–1293. [[CrossRef](#)]
35. Hasler, U.; Leroy, V.; Jeon, U.S.; Bouley, R.; Dimitrov, M.; Kim, J.A.; Brown, D.; Kwon, H.M.; Martin, P.Y.; Feraille, E. NF-kappaB modulates aquaporin-2 transcription in renal collecting duct principal cells. *J. Biol. Chem.* **2008**, *283*, 28095–28105. [[CrossRef](#)] [[PubMed](#)]
36. Küper, C.; Beck, F.X.; Neuhofer, W. Toll-like receptor 4 activates NF-κB and MAP kinase pathways to regulate expression of proinflammatory COX-2 in renal medullary collecting duct cells. *Am. J. Physiol. Renal Physiol.* **2012**, *302*, F38–F46. [[CrossRef](#)] [[PubMed](#)]
37. Kim, D.G.; Bae, G.S.; Jo, I.J.; Choi, S.B.; Kim, M.J.; Jeong, J.H.; Kang, D.G.; Lee, H.S.; Song, H.J.; Park, S.J. Guggulsterone attenuated lipopolysaccharide-induced inflammatory responses in mouse inner medullary collecting duct-3 cells. *Inflammation* **2016**, *39*, 87–95. [[CrossRef](#)] [[PubMed](#)]
38. Paragas, N.; Qiu, A.; Zhang, Q.; Samstein, B.; Deng, S.X.; Schmidt-Ott, K.M.; Viltard, M.; Yu, W.; Forster, C.S.; Gong, G.; et al. The Ngal reporter mouse detects the response of the kidney to injury in real time. *Nat. Med.* **2011**, *17*, 216–222. [[CrossRef](#)] [[PubMed](#)]
39. Schneider-Poetsch, T.; Ju, J.; Eyler, D.E.; Dang, Y.; Bhat, S.; Merrick, W.C.; Green, R.; Shen, B.; Liu, J.O. Inhibition of eukaryotic translation elongation by cycloheximide and lactimidomycin. *Nat. Chem. Biol.* **2010**, *6*, 209–217. [[CrossRef](#)]
40. Hoherl, K.; Schmidt, C.; Kurt, B.; Bucher, M. Inhibition of NF-kappaB ameliorates sepsis-induced downregulation of aquaporin-2/V2 receptor expression and acute renal failure in vivo. *Am. J. Physiol. Renal Physiol.* **2010**, *298*, F196–F204. [[CrossRef](#)]
41. Messeguer, X.; Escudero, R.; Farre, D.; Nunez, O.; Martinez, J.; Alba, M.M. PROMO: Detection of known transcription regulatory elements using species-tailored searches. *Bioinformatics* **2002**, *18*, 333–334. [[CrossRef](#)]
42. Farre, D.; Roset, R.; Huerta, M.; Adsuara, J.E.; Rosello, L.; Alba, M.M.; Messeguer, X. Identification of patterns in biological sequences at the ALGGEN server: PROMO and MALGEN. *Nucleic Acids Res.* **2003**, *31*, 3651–3653. [[CrossRef](#)]
43. Zhou, X.; Wang, H.; Burg, M.B.; Ferraris, J.D. Inhibitory phosphorylation of GSK-3beta by AKT, PKA, and PI3K contributes to high NaCl-induced activation of the transcription factor NFAT5 (TonEBP/OREBP). *Am. J. Physiol. Renal Physiol.* **2013**, *304*, F908–F917. [[CrossRef](#)] [[PubMed](#)]
44. Ferraris, J.D.; Williams, C.K.; Ohtaka, A.; Garcia-Perez, A. Functional consensus for mammalian osmotic response elements. *Am. J. Physiol.* **1999**, *276*, C667–C673. [[CrossRef](#)] [[PubMed](#)]
45. Khan, A.; Fornes, O.; Stigliani, A.; Gheorghe, M.; Castro-Mondragon, J.A.; van der Lee, R.; Bessy, A.; Cheneby, J.; Kulkarni, S.R.; Tan, G.; et al. JASPAR 2018: Update of the open-access database of transcription factor binding profiles and its web framework. *Nucleic Acids Res.* **2018**, *46*, D260–D266. [[CrossRef](#)] [[PubMed](#)]
46. Sheng, Z.; Wang, S.Z.; Green, M.R. Transcription and signalling pathways involved in BCR-ABL-mediated misregulation of 24p3 and 24p3R. *EMBO J.* **2009**, *28*, 866–876. [[CrossRef](#)] [[PubMed](#)]
47. Hasler, U.; Nielsen, S.; Feraille, E.; Martin, P.Y. Posttranscriptional control of aquaporin-2 abundance by vasopressin in renal collecting duct principal cells. *Am. J. Physiol. Renal Physiol.* **2006**, *290*, F177–F187. [[CrossRef](#)] [[PubMed](#)]
48. Lee, Y.C.; Lin, S.D.; Yu, H.M.; Chen, S.T.; Chu, S.T. Phosphorylation of the 24p3 protein secreted from mouse uterus in vitro and in vivo. *J. Protein Chem.* **2001**, *20*, 563–569. [[CrossRef](#)] [[PubMed](#)]
49. Correnti, C.; Strong, R.K. Mammalian siderophores, siderophore-binding lipocalins, and the labile iron pool. *J. Biol. Chem.* **2012**, *287*, 13524–13531. [[CrossRef](#)]
50. Gaeggeler, H.P.; Gonzalez-Rodriguez, E.; Jaeger, N.F.; Loffing-Cueni, D.; Norregaard, R.; Loffing, J.; Horisberger, J.D.; Rossier, B.C. Mineralocorticoid versus glucocorticoid receptor occupancy mediating aldosterone-stimulated sodium transport in a novel renal cell line. *J. Am. Soc. Nephrol.* **2005**, *16*, 878–891. [[CrossRef](#)]
51. Fila, M.; Brideau, G.; Morla, L.; Cheval, L.; Deschenes, G.; Doucet, A. Inhibition of K<sup>+</sup> secretion in the distal nephron in nephrotic syndrome: Possible role of albuminuria. *J. Physiol.* **2011**, *589*, 3611–3621. [[CrossRef](#)]
52. Mordasini, D.; Bustamante, M.; Rousselot, M.; Martin, P.Y.; Hasler, U.; Feraille, E. Stimulation of Na<sup>+</sup> transport by AVP is independent of PKA phosphorylation of the Na-K-ATPase in collecting duct principal cells. *Am. J. Physiol. Renal Physiol.* **2005**, *289*, F1031–F1039. [[CrossRef](#)]

53. Moeller, H.B.; Slengerik-Hansen, J.; Aroankins, T.; Assentoft, M.; MacAulay, N.; Moestrup, S.K.; Bhalla, V.; Fenton, R.A. Regulation of the Water Channel Aquaporin-2 via 14-3-3theta and -zeta. *J. Biol. Chem.* **2016**, *291*, 2469–2484. [[CrossRef](#)] [[PubMed](#)]
54. Nair, A.R.; Lee, W.K.; Smeets, K.; Swennen, Q.; Sanchez, A.; Thévenod, F.; Cuypers, A. Glutathione and mitochondria determine acute defense responses and adaptive processes in cadmium-induced oxidative stress and toxicity of the kidney. *Arch. Toxicol.* **2015**, *89*, 2273–2289. [[CrossRef](#)] [[PubMed](#)]
55. Bustin, S.A.; Benes, V.; Garson, J.A.; Hellemans, J.; Huggett, J.; Kubista, M.; Mueller, R.; Nolan, T.; Pfaffl, M.W.; Shipley, G.L.; et al. The MIQE guidelines: Minimum information for publication of quantitative real-time PCR experiments. *Clin. Chem.* **2009**, *55*, 611–622. [[CrossRef](#)] [[PubMed](#)]
56. Lam, Y.W.; Lamond, A.I. Isolation of nucleoli. In *Cell Biology: A Laboratory Handbook*, 3rd ed.; Celis, J.E., Ed.; Elsevier Academic Press: Burlington, MA, USA, 2006; Volume 2, pp. 103–108.
57. Bradford, M.M. A rapid and sensitive method for the quantitation of microgram quantities of protein utilizing the principle of protein-dye binding. *Anal. Biochem.* **1976**, *72*, 248–254. [[CrossRef](#)]
58. Schneider, C.A.; Rasband, W.S.; Eliceiri, K.W. NIH Image to ImageJ: 25 years of image analysis. *Nat. Methods* **2012**, *9*, 671–675. [[CrossRef](#)]
59. Wolff, N.A.; Abouhamed, M.; Verroust, P.J.; Thévenod, F. Megalin-dependent internalization of cadmium-metallothionein and cytotoxicity in cultured renal proximal tubule cells. *J. Pharmacol. Exp. Ther.* **2006**, *318*, 782–787. [[CrossRef](#)]



© 2019 by the authors. Licensee MDPI, Basel, Switzerland. This article is an open access article distributed under the terms and conditions of the Creative Commons Attribution (CC BY) license (<http://creativecommons.org/licenses/by/4.0/>).